# Coupled-channel analysis of the possible $D^{(*)}D^{(*)}$, $\bar{B}^{(*)}\bar{B}^{(*)}$ and $D^{(*)}\bar{B}^{(*)}$ molecular states

Ning Li[1],* Zhi-Feng Sun[2,3],† Xiang Liu[2,3],‡ and Shi-Lin Zhu[1,4]§

[1]*Department of Physics and State Key Laboratory of Nuclear Physics and Technology, Peking University, Beijing 100871, China*

[2]*School of Physical Science and Technology, Lanzhou University, Lanzhou 730000, China*

[3]*Research Center for Hadron and CSR Physics,Lanzhou University and Institute of Modern Physics of CAS, Lanzhou 730000, China*

[4]*Center of High Energy Physics, Peking University, Beijing 100871, China*

(Dated: November 22, 2012)

We perform a coupled-channel study of the possible deuteron-like molecules with two heavy flavor quarks, including the systems of $D^{(*)}D^{(*)}$ with double charm, $\bar{B}^{(*)}\bar{B}^{(*)}$ with double bottom and $D^{(*)}\bar{B}^{(*)}$ with both charm and bottom, within the one-boson-exchange model. In our study, we take into account the S-D mixing which plays an important role in the formation of the loosely bound deuteron, and particularly, the coupled-channel effect in the flavor space. According to our calculation, the states $D^{(*)}D^{(*)}[I(J^P) = 0(1^+)]$ and $(D^{(*)}D^{(*)})_s[J^P = 1^+]$ with double charm, the states $\bar{B}^{(*)}\bar{B}^{(*)}[I(J^P) = 0(1^+), 0(2^+), 1(0^+), 1(1^+), 1(2^+)]$, $(\bar{B}^{(*)}\bar{B}^{(*)})_s[J^P = 0^+, 1^+, 2^+]$ and $(\bar{B}^{(*)}\bar{B}^{(*)})_{ss}[J^P = 0^+, 1^+, 2^+]$ with double bottom, and the states $D^{(*)}\bar{B}^{(*)}[I(J^P) = 0(0^+), 0(1^+)]$ and $(D^{(*)}\bar{B}^{(*)})_s[J^P = 0^+, 1^+]$ with both charm and bottom are good molecule candidates. However, the existence of the states $D^{(*)}D^{(*)}[I(J^P) = 0(2^+)]$ with double charm and $D^{(*)}\bar{B}^{(*)}[I(J^P) = 1(1^+)]$ with both charm and bottom is ruled out.

PACS numbers: 14.40.Rt, 14.40.Lb, 12.39.Hg, 12.39.Pn

## I. INTRODUCTION

More and more experimental observations have stimulated the extensive discussions of exotic states. The molecular state explanation to the reported charmonium-like states $X, Y, Z$ becomes popular due to the fact that many charmonium-like states near the threshold of charmed meson pair, *i.e.*,

$$X(3872) \sim m_{D\bar{D}^*}, \quad Y(3930) \sim m_{D^*\bar{D}^*}$$
$$Y(4140) \sim m_{D_s^*\bar{D}_s^*}, \quad Y(4274) \sim m_{D_{s0}(2317)\bar{D}_s}.$$

And, in the past decade there is abundant literature with the study of the heavy flavor molecular states [1–23].

The concept of molecular state with hidden charm was first proposed by Voloshin and Okun thirty years ago and they studied the interaction between the charmed and anti-charmed mesons [24]. Later, De Rujula, Georgi and Glashow suggested that the observed $\psi(4040)$ is a $D^*\bar{D}^*$ molecule [25]. By the quark-pion interaction model, Törnqvist investigated the possible deuteron-like two meson bound states with $B\bar{B}^*$ or $B^*\bar{B}^*$ component [26, 27]. At present, carrying out the phenomenological study of the heavy flavor molecular state is still a hot research topic of hadron physics.

Usually, the hadron configurations mainly include

$$\text{Hadron}\begin{cases}\text{Meson}: & q\bar{q},\ Q\bar{q},\ Q\bar{Q}\\ \text{Baryon}: & qqq,\ Qqq,\ QQq,\ \ldots\\ \text{Exotic state}: & \begin{cases}\text{Molecular state}\\ \text{Hybrid}\\ \text{Glueball}\\ \ldots\end{cases}\end{cases},$$

where $q$ and $Q$ denote the light $(u, d, s)$ and heavy $(c, b)$ quarks, respectively. Among the conventional baryon states, the baryons with double charm or double bottom is of the $QQq$ configuration. The SELEX Collaboration reported the first observation of a doubly charmed baryon $\Xi_{cc}^+$ in its charged decay mode $\Xi_{cc}^+ \to \Lambda_c^+ K^- \pi^+$ [28] and confirmed it in the decay mode $\Xi_{cc}^+ \to pD^+K^-$ [29]. However, later the BABAR Collaboration searched for $\Xi_{cc}^+$ in the final states $\Lambda_c^+ K^-\pi^+$ and $\Xi_c^0\pi^+$, and $\Xi_{cc}^{++}$ in the final states $\Lambda_c^+ K^-\pi^+\pi^-$ and $\Xi_c^0\pi^+\pi^+$, and found no evidence for the production of the doubly charmed baryons [30]. The Belle Collaboration reported no evidence for the doubly charmed baryons in the final state $\Lambda_c^+ K^-\pi^+$, either [31]. Although these doubly charmed baryons were not confirmed by BABAR and BELLE, it is still an interesting research topic to search for such doubly charmed baryons experimentally.

Besides the doubly heavy flavor baryons, it is also very interesting to study other systems with two heavy flavor quarks. The heavy flavor molecular state with two charm quarks provides another approach to investigate the hadron states with double charm. For this kind of hadron, its typical configuration is $[c\bar{q}][c\bar{q}]$. To answer whether there exist such heavy flavor molecular states with double charm or not, in this paper we apply the one-boson-exchange (OBE) model to perform a dynamic calculation of their mass spectroscopy. This study is not only a natural extension of the previous work of the heavy flavor molecular state with hidden charm, but also provides new insight into exploring the hadron states with double charm. Besides the hadron states with double charm, we also investigate the hadron states with double bottom and the hadron states with both charm and bottom.

This paper is organized as follows. After the introduction, we present the derivation of the effective potential in Section II. We summarize our numerical results and perform some analysis in Section III and draw some conclusions in Section IV. We also give some useful formulas in the Appendix.

*Electronic address: leening@pku.edu.cn
†Electronic address: sunzhif09@lzu.edu.cn
‡Electronic address: xiangliu@lzu.edu.cn
§Electronic address: zhusl@pku.edu.cn

## II. FORMALISM

### A. The lagrangians and the coupling constants

In the present paper, we investigate the possible molecules of $(D^{(*)}D^{(*)})$ with double charm, $(B^{(*)}B^{(*)})$ with double bottom and $(D^{(*)}B^{(*)})$ with both charm and bottom. In our study, we take into account the S-D mixing which plays an important role in the formation of the loosely bound deuteron and, particularly, the coupled-channel effects in the flavor space. We study the systems with total angular momentum $J \leq 2$. We list the channels for different systems in Tables I-II.

The Lagrangians under the heavy quark symmetry and the SU(3)-flavor symmetry read [32–35]

$$\begin{aligned}
\mathcal{L}_{HH\mathcal{M}} &= ig\mathrm{Tr}\left[H_b^{(Q)}\gamma_\mu\gamma_5 A^\mu_{ba}\bar{H}_a^{(Q)}\right], && (1)\\
\mathcal{L}_{HHV} &= i\beta\mathrm{Tr}\left[H_b^{(Q)}v_\mu(V^\mu_{ba}-\rho^\mu_{ba})\bar{H}_a^{(Q)}\right] \\
&\quad +i\lambda\mathrm{Tr}\left[H_b^{(Q)}\sigma_{\mu\nu}F^{\mu\nu}(\rho)_{ba}\bar{H}_a^{(Q)}\right], && (2)\\
\mathcal{L}_{HH\sigma} &= g_s\mathrm{Tr}\left[H_a^{(Q)}\sigma\bar{H}_a^{(Q)}\right], && (3)
\end{aligned}$$

where $H^{(Q)}$ and $\bar{H}^{(Q)}$ are defined as

$$H_a^{(Q)} = \frac{1+\not{v}}{2}[P_a^{*\mu}\gamma_\mu - P_a\gamma_5] \quad (4)$$

and

$$\bar{H}_a^{(Q)} \equiv \gamma_0 H^{(Q)\dagger}\gamma_0 = [P_a^{*\mu}\gamma_\mu + P_a\gamma_5]\frac{1+\not{v}}{2} \quad (5)$$

with $P_a^* = (D^{*0}, D^{*+}, D_s^{*+})$ or $(B^{*-}, \bar{B}^{*0}, \bar{B}_s^{*0})$ being the charmed or antibottomed vector mesons and $P = (D^0, D^+, D_s^+)$ or $(B^-, \bar{B}^0, \bar{B}_s^0)$ being the charmed or anti-bottomed pseudoscalar mesons. The trace acts on the gamma matrices. The axial-current $A^\mu$ is defined as $A^\mu \equiv \frac{1}{2}\left(\xi^\dagger\partial^\mu\xi - \xi\partial^\mu\xi^\dagger\right) = \frac{i}{f_\pi}\partial^\mu\mathcal{M}+\ldots$ where $\xi \equiv e^{\frac{i\mathcal{M}}{f_\pi}}$ with $\mathcal{M}$ being the exchanged pseudoscalar meson matrix given in Eq. (6). The vector current $V^\mu$ is defined as $V^\mu \equiv \frac{1}{2}\left(\xi^\dagger\partial^\mu\xi + \xi\partial^\mu\xi^\dagger\right)$. In the heavy quark limit, the heavy meson velocity is adopted as $v^\mu = (1,0,0,0)$. $F_{\mu\nu}(\rho) \equiv \partial_\mu\rho_\nu - \partial_\nu\rho_\mu - \left[\rho_\mu, \rho_\nu\right]$ where $\rho_\mu = \frac{ig_v}{\sqrt{2}}\hat{\rho}_\mu$ with $\hat{\rho}$ being the exchanged vector meson matrix given in Eq. 7. Expanding the Lagrangians given in Eqs. (1-3), we list the specific expressions in Eqs. (8-14).

$$\mathcal{M} = \begin{pmatrix} \frac{1}{\sqrt{2}}\pi^0 + \frac{\eta}{\sqrt{6}} & \pi^+ & K^+ \\ \pi^- & -\frac{1}{\sqrt{2}}\pi^0 + \frac{\eta}{\sqrt{6}} & K^0 \\ K^- & \bar{K}^0 & -\frac{2}{\sqrt{6}}\eta \end{pmatrix}, \quad (6)$$

$$\hat{\rho}^\mu = \begin{pmatrix} \frac{\rho^0}{\sqrt{2}} + \frac{\omega}{\sqrt{2}} & \rho^+ & K^{*+} \\ \rho^- & -\frac{\rho^0}{\sqrt{2}} + \frac{\omega}{\sqrt{2}} & K^{*0} \\ K^{*-} & \bar{K}^{*0} & \phi \end{pmatrix}^\mu. \quad (7)$$

$$\begin{aligned}
\mathcal{L}_{P^*P^*\mathcal{M}} &= -i\frac{2g}{f_\pi}\varepsilon_{\alpha\mu\nu\lambda}v^\alpha P_b^{*\mu}P_a^{*\lambda\dagger}\partial^\nu M_{ba}, && (8)\\
\mathcal{L}_{P^*P\mathcal{M}} &= -\frac{2g}{f_\pi}\left(P_b P_{a\lambda}^{*\dagger} + P_{b\lambda}^* P_a^\dagger\right)\partial^\lambda M_{ba}, && (9)
\end{aligned}$$

$$\begin{aligned}
\mathcal{L}_{PPV} &= -\sqrt{2}\beta g_V P_b P_a^\dagger v\cdot\hat{\rho}_{ba}, && (10)\\
\mathcal{L}_{P^*PV} &= -2\sqrt{2}\lambda g_V v^\lambda\varepsilon_{\lambda\mu\alpha\beta}\left(P_b P_a^{*\mu\dagger} + P_b^{*\mu}P_a^\dagger\right)\left(\partial^\alpha\hat{\rho}^\beta\right)_{ba}, && (11)\\
\mathcal{L}_{P^*P^*V} &= \sqrt{2}\beta g_V P_b^*\cdot P_a^{*\dagger}v\cdot\hat{\rho}_{ba} \\
&\quad -i2\sqrt{2}\lambda g_V P_b^{*\mu}P_a^{*\nu\dagger}\left(\partial_\mu\hat{\rho}_\nu - \partial_\nu\hat{\rho}_\mu\right)_{ba}, && (12)
\end{aligned}$$

$$\begin{aligned}
\mathcal{L}_{PP\sigma} &= -2g_s P_b P_b^\dagger\sigma, && (13)\\
\mathcal{L}_{P^*P^*\sigma} &= 2g_s P_b^*\cdot P_b^{*\dagger}\sigma, && (14)
\end{aligned}$$

In the above, $f_\pi = 132$ MeV is the pion decay constant. The coupling constants $g$ was studied by many theoretical approaches, such as quark model [33] and QCD sum rule [36, 37]. In our study, we take the experimental result of the CLEO Collaboration, $g = 0.59 \pm 0.07 \pm 0.01$, which was extracted from the full width of $D^{*+}$ [38]. For the coupling constants relative to the vector meson exchange, we adopt the values $g_v = 5.8$ and $\beta = 0.9$ which were determined by the vector meson dominance mechanism, and $\lambda = 0.56$ GeV$^{-1}$ which was obtained by matching the form factor predicted by the effective theory approach with that obtained by the light cone sum rule and the lattice QCD simulation [39, 40]. The coupling constant for the scalar meson exchange is $g_s = g_\pi/(2\sqrt{6})$ [10] with $g_\pi = 3.73$. We take the masses of the heavy mesons and the exchanged light mesons from PDG [41] and summarize them in Table III.

### B. The derivation of the effective potentials

Using the lagrangians given in Eqs. (8-14), one can easily deduce the effective potentials in the momentum space. Taking into account the structure effect of the heavy mesons, we introduce a monopole form factor

$$F(q) = \frac{\Lambda^2 - m_{ex}^2}{\Lambda^2 - q^2} \quad (15)$$

at each vertex. Here, $\Lambda$ is the cutoff parameter and $m_{ex}$ is the mass of the exchanged meson. Making fourier transformation

$$V(r) = \frac{1}{(2\pi)^3}\int d\mathbf{q}^3 e^{-i\mathbf{q}\cdot\mathbf{r}}V(\mathbf{q})F^2(\mathbf{q}) \quad (16)$$

one can obtain the effective potentials in the coordinate space. In Eqs. (18-31), we list the specific expressions of the effective subpotentials which are flavor-independent. The effective

TABLE I: The different channels for the $D^{(*)}D^{(*)}$ systems, and similarly, for the $\bar{B}^{(*)}\bar{B}^{(*)}$. $S$ is the strangeness while $I$ stands for the isospin of the systems. "×" means the corresponding state dose not exist due to the symmetry. For simplicity, we adopt the shorthand notations, $[DD^*]_- \equiv \frac{1}{\sqrt{2}}(DD^* - D^*D)$ and $[DD^*]_+ \equiv \frac{1}{\sqrt{2}}(DD^* + D^*D)$.

| | | | Channels | | | | | | |
|---|---|---|---|---|---|---|---|---|---|
| $S$ | $I$ | $J^P$ | 1 | 2 | 3 | 4 | 5 | 6 | 7 |
| 0 | 0 | $0^+$ | | | | × | | | |
| | | $1^+$ | $[DD^*]_-(^3S_1)$ | $[DD^*]_-(^3D_1)$ | $D^*D^*(^3S_1)$ | $D^*D^*(^3D_1)$ | | | |
| | | $2^+$ | $[DD^*]_-(^3D_2)$ | $D^*D^*(^3D_2)$ | | | | | |
| | 1 | $0^+$ | $DD(^1S_0)$ | $D^*D^*(^1S_0)$ | $D^*D^*(^5D_0)$ | | | | |
| | | $1^+$ | $[DD^*]_+(^3S_1)$ | $[DD^*]_+(^3D_1)$ | $D^*D^*(^5D_1)$ | | | | |
| | | $2^+$ | $D^*D^*(^5S_2)$ | $D^*D^*(^1D_2)$ | $D^*D^*(^5D_2)$ | | | | |
| 1 | $\frac{1}{2}$ | $0^+$ | $DD_s(^1S_0)$ | $D^*D_s^*(^1S_0)$ | $D^*D_s^*(^5D_0)$ | | | | |
| | | $1^+$ | $DD_s^*(^3S_1)$ | $DD_s^*(^3D_1)$ | $D^*D_s(^3S_1)$ | $D^*D_s(^3D_1)$ | $D^*D_s^*(^3S_1)$ | $D^*D_s^*(^3D_1)$ | $D^*D_s^*(^5D_1)$ |
| | | $2^+$ | $D^*D_s^*(^5S_2)$ | $D^*D_s^*(^1D_2)$ | $D^*D_s^*(^5D_2)$ | | | | |
| 2 | 0 | $0^+$ | $D_sD_s(^1S_0)$ | $D_s^*D_s^*(^1S_0)$ | $D_s^*D_s^*(^5D_0)$ | | | | |
| | | $1^+$ | $[D_sD_s^*]_+(^3S_1)$ | $[D_sD_s^*]_+(^3D_1)$ | $D_s^*D_s^*(^5D_1)$ | | | | |
| | | $2^+$ | $D_s^*D_s^*(^5S_2)$ | $D_s^*D_s^*(^1D_2)$ | $D_s^*D_s^*(^5D_2)$ | | | | |

TABLE II: The different channels for the $D^{(*)}\bar{B}^{(*)}$ systems. "$S$" is the strangeness of the corresponding system while "$I$" stands for the isospin of the state.

| | | | Channels | | | | | | | | | |
|---|---|---|---|---|---|---|---|---|---|---|---|---|
| $S$ | $I$ | $J^P$ | 1 | 2 | 3 | 4 | 5 | 6 | 7 | 8 | 9 | 10 |
| 0 | 0 | $0^+$ | $D\bar{B}(^1S_0)$ | $D^*\bar{B}^*(^1S_0)$ | $D^*\bar{B}^*(^5D_0)$ | | | | | | | |
| | | $1^+$ | $D\bar{B}^*(^3S_1)$ | $D\bar{B}^*(^3D_1)$ | $D^*\bar{B}(^3S_1)$ | $D^*\bar{B}(^3D_1)$ | $D^*\bar{B}^*(^3S_1)$ | $D^*\bar{B}^*(^3D_1)$ | $D^*\bar{B}^*(^5D_1)$ | | | |
| | | $2^+$ | $D^*\bar{B}^*(^5S_2)$ | $D^*\bar{B}^*(^1D_2)$ | $D^*\bar{B}^*(^5D_2)$ | | | | | | | |
| | 1 | $0^+$ | $D\bar{B}(^1S_0)$ | $D^*\bar{B}^*(^1S_0)$ | $D^*\bar{B}^*(^5D_0)$ | | | | | | | |
| | | $1^+$ | $D\bar{B}^*(^3S_1)$ | $D\bar{B}^*(^3D_1)$ | $D^*\bar{B}(^3S_1)$ | $D^*\bar{B}(^3D_1)$ | $D^*\bar{B}^*(^3S_1)$ | $D^*\bar{B}^*(^3D_1)$ | $D^*\bar{B}^*(^5D_1)$ | | | |
| | | $2^+$ | $D^*\bar{B}^*(^5S_2)$ | $D^*\bar{B}^*(^1D_2)$ | $D^*\bar{B}^*(^5D_2)$ | | | | | | | |
| 1 | $\frac{1}{2}$ | $0^+$ | $D\bar{B}_s(^1S_0)$ | $D_s\bar{B}(^1S_0)$ | $D^*\bar{B}_s^*(^1S_0)$ | $D_s^*\bar{B}^*(^1S_0)$ | $D^*\bar{B}_s^*(^5D_0)$ | $D_s^*\bar{B}^*(^5D_0)$ | | | | |
| | | $1^+$ | $D_s\bar{B}^*(^3S_1)$ | $D\bar{B}_s^*(^3S_1)$ | $D_s^*\bar{B}(^3S_1)$ | $D^*\bar{B}_s(^3S_1)$ | $D_s^*\bar{B}^*(^3S_1)$ | $D^*\bar{B}_s^*(^3S_1)$ | $D_s\bar{B}^*(^3D_1)$ | $D\bar{B}_s^*(^3D_1)$ | $D_s^*\bar{B}(^3D_1)$ | $D^*\bar{B}_s(^3D_1)$ |
| | | $2^+$ | $D_s^*\bar{B}^*(^5S_2)$ | $D^*\bar{B}_s^*(^5S_2)$ | $D_s^*\bar{B}^*(^1D_2)$ | $D^*\bar{B}_s^*(^1D_2)$ | $D_s^*\bar{B}^*(^5D_2)$ | $D^*\bar{B}_s^*(^5D_2)$ | | | | |
| 2 | 0 | $0^+$ | $D_s\bar{B}_s(^1S_0)$ | $D_s^*\bar{B}_s^*(^1S_0)$ | $D_s^*\bar{B}_s^*(^5D_0)$ | | | | | | | |
| | | $1^+$ | $D_s\bar{B}_s^*(^3S_1)$ | $D_s\bar{B}_s^*(^3D_1)$ | $D_s^*\bar{B}_s(^3S_1)$ | $D_s^*\bar{B}_s(^3D_1)$ | $D_s^*\bar{B}_s^*(^3S_1)$ | $D_s^*\bar{B}_s^*(^3D_1)$ | $D_s^*\bar{B}_s^*(^5D_1)$ | | | |
| | | $2^+$ | $D_s^*\bar{B}_s^*(^5S_2)$ | $D_s^*\bar{B}_s^*(^1D_2)$ | $D_s^*\bar{B}_s^*(^5D_2)$ | | | | | | | |

potential used in our calculation is the product of the flavor-independent subpotentials and the isospin-dependent coefficients which are summarized in the Appendix VI. The flavor-independent subpotentials are

$$V_\sigma^a(r) = -g_s^2 H_0(\Lambda, q_0, m_\sigma, r), \quad (17)$$

$$V_v^a(r) = \frac{\beta^2 g_V^2}{2} H_0(\Lambda, q_0, m_v, r), \quad (18)$$

for the process $PP \to PP$,

$$V_{p/\sigma/v}^b(r) = 0 \quad (19)$$

for the scattering process $PP \to PP^*$,

$$V_p^c(r) = \frac{g^2}{f_\pi^2}\Big[H_3(\Lambda, q_0, m_p, r)T(\boldsymbol{\epsilon}_3^\dagger, \boldsymbol{\epsilon}_4^\dagger) + \frac{1}{3}H_1(\Lambda, q_0, m_p, r)S(\boldsymbol{\epsilon}_3^\dagger, \boldsymbol{\epsilon}_4^\dagger)\Big] \quad (20)$$

TABLE III: The masses of the heavy mesons and the exchanged light mesons taken from the PDG [41]. In our study, we keep the isospin symmetry. For the isospin multiplet, we use the averaged mass in our study.

| Heavy Mesons | Mass (MeV) | Exchanged Mesons | Mass (MeV) |
|---|---|---|---|
| $D^{\pm}$ | 1869.60 | $\pi^{\pm}$ | 139.57 |
| $D^{0}$ | 1864.83 | $\pi^{0}$ | 134.98 |
| $D^{*\pm}$ | 2010.25 | $\eta$ | 547.85 |
| $D^{*0}$ | 2006.96 | $\rho$ | 775.49 |
| $D_s^{\pm}$ | 1968.47 | $\omega$ | 782.65 |
| $D_s^{*\pm}$ | 2112.3 | $\phi$ | 1019.46 |
| $B^{*}$ | 5325.1 | $\sigma$ | 600 |
| $B^{\pm}$ | 5279.17 | $K^{\pm}$ | 493.67 |
| $B^{0}$ | 5279.50 | $K^{0}$ | 497.61 |
| $B_s^{0}$ | 5366.3 | $K^{*\pm}$ | 891.66 |
| $B_s^{*}$ | 5415.4 | $K^{*0}$ | 895.94 |

$$V_{\nu}^{c}(r) = -2\lambda^2 g_V^2\Big[H_3(\Lambda,q_0,m_\nu,r)T(\boldsymbol{\epsilon}_3^{\dagger},\boldsymbol{\epsilon}_4^{\dagger}) -\frac{2}{3}H_1(\Lambda,q_0,m_\nu,r)S(\boldsymbol{\epsilon}_3^{\dagger},\boldsymbol{\epsilon}_4^{\dagger})\Big] \quad (21)$$

for the scattering process $PP \to P^*P^*$,

$$V_{\sigma}^{d}(r) = -g_s^2 H_0(\Lambda,q_0,m_\sigma,r)S(\boldsymbol{\epsilon}_4^{\dagger},\boldsymbol{\epsilon}_2) \quad (22)$$

$$V_{\nu}^{d}(r) = \frac{\beta^2 g_V^2}{2}H_0(\Lambda,q_0,m_\nu,r)S(\boldsymbol{\epsilon}_4^{\dagger},\boldsymbol{\epsilon}_2) \quad (23)$$

for the scattering process $PP^* \to PP^*$,

$$V_{\pi}^{e}(r) = \frac{g^2}{f_\pi^2}\Big[M_3(\Lambda,q_0,m_\pi,r)T(\boldsymbol{\epsilon}_3^{\dagger},\boldsymbol{\epsilon}_2) +\frac{1}{3}M_1(\Lambda,q_0,m_\pi,r)S(\boldsymbol{\epsilon}_3^{\dagger},\boldsymbol{\epsilon}_2)\Big] \quad (24)$$

$$V_{\pi/\eta/K}^{e}(r) = \frac{g^2}{f_\pi^2}\Big[H_3(\Lambda,q_0,m_{\pi/\eta/K},r)T(\boldsymbol{\epsilon}_3^{\dagger},\boldsymbol{\epsilon}_2) +\frac{1}{3}H_1(\Lambda,q_0,m_{\pi/\eta/K},r)S(\boldsymbol{\epsilon}_3^{\dagger},\boldsymbol{\epsilon}_2)\Big] \quad (25)$$

$$V_{\nu}^{e}(r) = -2\lambda^2 g_V^2\Big[H_3(\Lambda,q_0,m_\nu,r)T(\boldsymbol{\epsilon}_3^{\dagger},\boldsymbol{\epsilon}_2) -\frac{2}{3}H_1(\Lambda,q_0,m_\nu,r)S(\boldsymbol{\epsilon}_3^{\dagger},\boldsymbol{\epsilon}_2)\Big] \quad (26)$$

for the scattering process $PP^* \to P^*P$,

$$V_{p}^{f}(r) = \frac{g^2}{f_\pi^2}\Big[H_3(\Lambda,q_0,m_p,r)T(\boldsymbol{\epsilon}_3^{\dagger},i\boldsymbol{\epsilon}_4^{\dagger}\times\boldsymbol{\epsilon}_2) +\frac{1}{3}H_1(\Lambda,q_0,m_p,r)T(\boldsymbol{\epsilon}_3^{\dagger},i\boldsymbol{\epsilon}_4^{\dagger}\times\boldsymbol{\epsilon}_2)\Big] \quad (27)$$

$$V_{\nu}^{f}(r) = 2\lambda^2 g_V^2\Big\{H_3(\Lambda,q_0,m_\nu,r) \times\Big[T(i\boldsymbol{\epsilon}_3^{\dagger}\times\boldsymbol{\epsilon}_4^{\dagger},\boldsymbol{\epsilon}_2)-T(i\boldsymbol{\epsilon}_3^{\dagger}\times\boldsymbol{\epsilon}_2^{\dagger},\boldsymbol{\epsilon}_4^{\dagger})\Big] +\frac{1}{3}H_1(\Lambda,q_0,m_\nu,r) \times\Big[S(i\boldsymbol{\epsilon}_3^{\dagger}\times\boldsymbol{\epsilon}_4^{\dagger},\boldsymbol{\epsilon}_2)-S(i\boldsymbol{\epsilon}_3^{\dagger}\times\boldsymbol{\epsilon}_2^{\dagger},\boldsymbol{\epsilon}_4^{\dagger})\Big]\Big\} \quad (28)$$

for the scattering process $PP^* \to P^*P^*$, and

$$V_{p}^{h}(r) = \frac{g^2}{f_\pi^2}\Big[H_3(\Lambda,q_0,m_p,r)T\left(i\boldsymbol{\epsilon}_3^{\dagger}\times\boldsymbol{\epsilon}_1,i\boldsymbol{\epsilon}_4^{\dagger}\times\boldsymbol{\epsilon}_2\right) +\frac{1}{3}H_1(\Lambda,q_0,m_p,r)S\left(i\boldsymbol{\epsilon}_3^{\dagger}\times\boldsymbol{\epsilon}_1,i\boldsymbol{\epsilon}_4^{\dagger}\times\boldsymbol{\epsilon}_2\right)\Big] \quad (29)$$

$$V_{\sigma}^{h}(r) = -g_s^2 H_0(\Lambda,q_0,m_\sigma,r)C\left(i\boldsymbol{\epsilon}_3^{\dagger}\times\boldsymbol{\epsilon}_1,i\boldsymbol{\epsilon}_4^{\dagger}\times\boldsymbol{\epsilon}_2\right) \quad (30)$$

$$V_{\nu}^{h}(r) = \frac{\beta^2 g_V^2}{2}H_0(\Lambda,q_0,m_\nu,r)C\left(i\boldsymbol{\epsilon}_3^{\dagger}\times\boldsymbol{\epsilon}_1,i\boldsymbol{\epsilon}_4^{\dagger}\times\boldsymbol{\epsilon}_2\right) -2\lambda^2 g_V^2\Big[H_3(\Lambda,q_0,m_\nu,r)T\left(i\boldsymbol{\epsilon}_3^{\dagger}\times\boldsymbol{\epsilon}_1,i\boldsymbol{\epsilon}_4^{\dagger}\times\boldsymbol{\epsilon}_2\right) -\frac{2}{3}H_1(\Lambda,q_0,m_\nu,r)S\left(i\boldsymbol{\epsilon}_3^{\dagger}\times\boldsymbol{\epsilon}_1,i\boldsymbol{\epsilon}_4^{\dagger}\times\boldsymbol{\epsilon}_2\right)\Big] \quad (31)$$

for the scattering process $P^*P^* \to P^*P^*$. To obtain the effective potentials $V^g(r)$ for the process $P^*P \to P^*P^*$, one just needs to make the following changes

$$\begin{aligned} &\boldsymbol{\epsilon}_3^{\dagger}\to\boldsymbol{\epsilon}_4^{\dagger}, \qquad i\boldsymbol{\epsilon}_4^{\dagger}\times\boldsymbol{\epsilon}_2\to i\boldsymbol{\epsilon}_3^{+}\times\boldsymbol{\epsilon}_1^{\dagger},\\ &\boldsymbol{\epsilon}_2\to\boldsymbol{\epsilon}_1, \qquad i\boldsymbol{\epsilon}_3^{\dagger}\times\boldsymbol{\epsilon}_4^{\dagger}\to i\boldsymbol{\epsilon}_4^{\dagger}\times\boldsymbol{\epsilon}_3^{\dagger},\\ &\boldsymbol{\epsilon}_4^{\dagger}\to\boldsymbol{\epsilon}_3^{\dagger}, \qquad i\boldsymbol{\epsilon}_3^{\dagger}\times\boldsymbol{\epsilon}_2\to i\boldsymbol{\epsilon}_4^{\dagger}\times\boldsymbol{\epsilon}_1, \end{aligned} \quad (32)$$

in Eqs.( 27)-(28). Functions $H_0$, $H_1$, $H_3$, $M_1$ and $M_3$ are given in the Appendix. Operator $C$, the generalized tensor operator $T$ and spin-spin operator $S$ are defined as

$$C(a,b) = ab, \quad (33)$$

$$T(\boldsymbol{a},\boldsymbol{b}) = \frac{3\boldsymbol{a}\cdot\boldsymbol{r}\boldsymbol{b}\cdot\boldsymbol{r}}{r^2}-\boldsymbol{a}\cdot\boldsymbol{b}, \quad (34)$$

$$S(\boldsymbol{a},\boldsymbol{b}) = \boldsymbol{a}\cdot\boldsymbol{b}. \quad (35)$$

Due to the large mass gap between the mesons $D(D^0,D^+)$, $D_s^+$, $D^*(D^{*0},D^{*+})$ and $D_s^{*+}$ (similarly, in the bottom sector), it is necessary to adopt the nonzero time component of the transferred momentum for some scattering processes. We present the $q_0$s used in our calculation in the Appendix. Notice that $m_{D^*}-m_D > m_\pi$ leads to the complex potential for the scattering process $DD^* \to D^*D$, and we take its real part which has an oscillation form, see Eq. (24).

## III. NUMERICAL RESULTS

Using the potentials given in the subsection II B, we solve the coupled-channel Schrödinger equation and summarize the numerical results which include the binding energy (B.E.), the system mass (M), the root-mean-square radius ($r_{rms}$) and the probability of the individual channel ($P_i$) in Tables IV, V, VII, VIII, IXand X.

### A. The Numerical Results for Systems with Strangeness $S = 0$

For the systems with strangeness $S = 0$, in order to highlight the role of the long-range pion exchange in the formation of the loosely bound state, we first give the numerical results with the pion-exchange potential alone, which are marked

with OPE, and then with the heavier eta, sigma, rho and omega exchanges as well as the pion exchange, which are marked with OBE, see Tables IV, V and VI.

### 1. $D^{(*)}D^{(*)}$

The state $D^{(*)}D^{(*)}[I(J^P) = 0(0^+)]$ is forbidden because the present boson system should satisfy the Boson-Einstein statistic. However, the state $D^{(*)}D^{(*)}[I(J^P) = 0(1^+)]$ is very interesting. Using the long-range pion exchange potential, we obtain a loosely bound state with a reasonable cutoff. For our present $D^{(*)}D^{(*)}[I(J^P) = 0(1^+)]$ state, with the cutoff parameter fixed larger than 1.05 GeV, the long-range pion exchange is strong enough to form the loosely bound state. If we set the cutoff parameter to be 1.05 GeV, the binding energy relative to the $DD^*$ threshold is 1.24 MeV and the corresponding root-mean-square radius is 3.11 fm which is comparable to the size of the deuteron (about 2.0 fm). The dominant channel is $[DD^*]_-(^3S_1)$, with a probability 96.39%. With such a large mass gap (about 140 MeV) between the threshold of $DD^*$ and that of $D^*D^*$, the contribution of the state $D^*D^*(^3S_1)$ is 2.79%. However, the probability of the D-wave is around 1%. When we tune the cutoff to be 1.20 GeV, the binding energy is 20.98 MeV and the root-mean-square radius changes into 0.84 fm. When we use the one-boson-exchange potential, we notice that the binding becomes deeper. For example, if the cutoff is fixed at 1.10 GeV, the binding energy is 4.63 MeV with OPE potential. However, it changes into 42.82 GeV with the OBE potential for the same cutoff, see Table IV. We also plot the potentials in Fig. 1. From the potentials, one can see that the heavier rho and omega exchange cancel each other significantly, and the residual interaction is helpful to strengthen the binding. The present meson exchange approach strongly suggests $D^{(*)}D^{(*)}[I(J^P) = 0(1^+)]$ to be a molecule.

We should mention that in the calculation of the $X(3872)$ one also obtained a bound $D\bar{D}^*$ state with quantum numbers $I(J^{PC}) = 0(1^{++})$ using the OPE potential [42, 44]. One may be confused since the difference between the potential of the $DD^*$ system and that of the $D\bar{D}^*$ system is the G-parity of the exchanged meson while the pion has an odd G-parity. Actually, the iso-singlet $D\bar{D}^*$ system has two C-parity states, one with even C-parity ($C = +$) and the other with odd C-parity ($C = -$). And, the interaction of our present $DD^*$ system relates to that of the odd C-parity but not the even C-parity $D\bar{D}^*$ state via the G-parity rule.

We obtain no binding solutions for the state $D^{(*)}D^{(*)}[I(J^P) = 0(2^+)]$ even if we tune the cutoff parameter as high as 3.0 GeV. Therefore, the existence of the state $D^{(*)}D^{(*)}[I(J^P) = 0(2^+)]$ as a molecule is ruled out within the present meson exchange approach.

For the state $D^{(*)}D^{(*)}[I(J^P) = 1(0^+)]$, with the cutoff less than 3.0 GeV, the long-range pion exchange is not sufficient to form the bound state. However, when we add the heavier eta, sigma, rho and omega exchanges and tune the cutoff to be 2.64 MeV, a bound state with mass 3730.17 MeV appears. The binding energy relative to the $DD$ threshold is 2.64 MeV and the corresponding root-mean-square radius is 1.38 fm. The

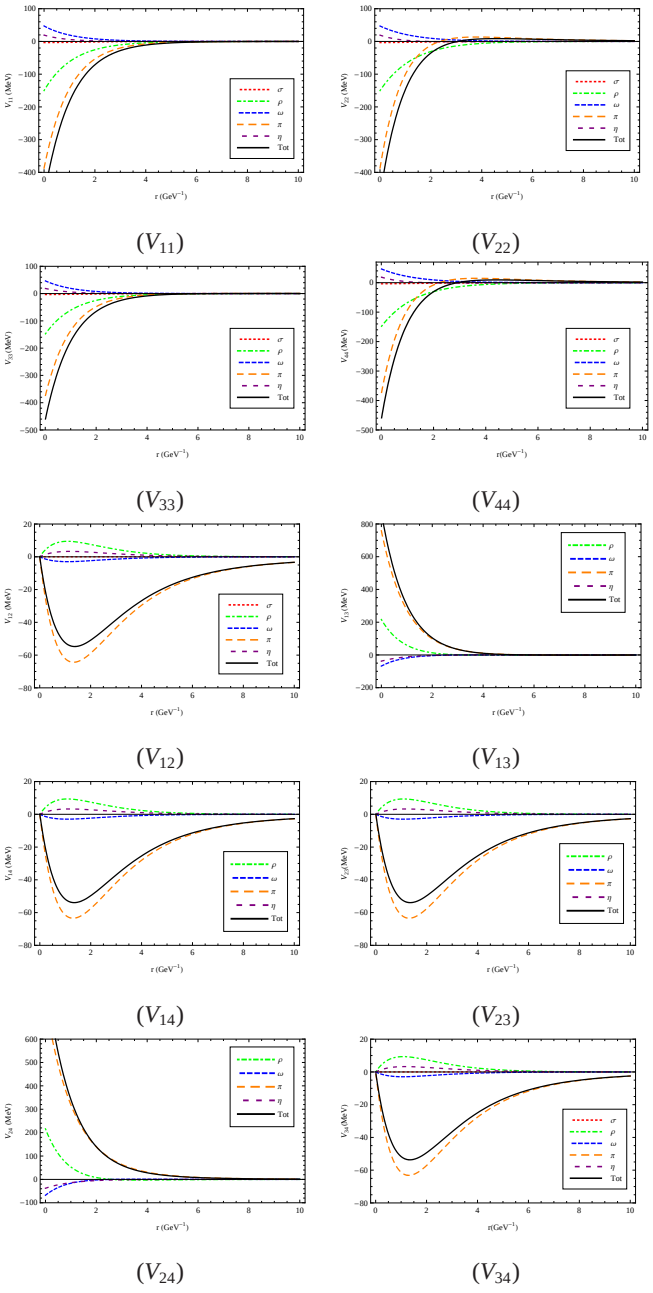


FIG. 1: Color online. The effective potentials for the state $D^{(*)}D^{(*)}[I(J^P) = 0(1^+)]$ with cutoff = 1.00 GeV.

channel $DD(^1S_0)$ with a probability of 91.47% dominates this state. The probability of the channel $D^*D^*(^5D_0)$ is very small, only 0.07%.

Just as the $J^P = 0^+$ case, with the pion-exchange potential alone we obtain no binding solutions for the state $D^{(*)}D^{(*)}[I(J^P) = 1(1^+)]$ with the cutoff parameter less than 3.0 GeV. When we use the OBE potential and tune the cutoff to be 2.48 GeV, we obtain a bound $D^{(*)}D^{(*)}[I(J^P) = 1(1^+)]$ state with mass 3875.58 MeV. The binding energy relative to the $DD^*$ threshold is 0.27 MeV and the corresponding root-mean-square radius is 5.81 fm. The dominant channel is

$[DD^*]_+(^3S_1)$, with a probability of 99.92%.

For the state $D^{(*)}D^{(*)}[I(J^P) = 1(2^+)]$, it is necessary to mention that there are five channels $DD(^1D_2)$, $[DD^*]_+(^3D_2)$, $D^*D^*(^5S_2)$, $D^*D^*(^1D_2)$ and $D^*D^*(^5D_2)$, with the quantum numbers $I(J^P) = 1(2^+)$. If we consider all the five channels, with the OBE potential we obtain a bound state with the cutoff parameter fixed to be 2.84 GeV. The binding energy relative to the $DD$ threshold is 12.93 MeV. Surprisingly, the corresponding root-mean-square radius is as small as 0.22 fm. The dominant channel is $D^*D^*(^5S_2)$, with a probability of 99.5%. However, the probability of the channel $DD(^1D_2)$ is so small as 0.04%, which tells us that this is not a loosely bound $DD$ state but a deeply bound $D^*D^*$ state. With so tight a bound state, the present meson-exchange model dose not work. Therefore, we omit the channels $DD(^3D_2)$ and $[DD^*]_+(^3D_2)$ and keep the three $D^*D^*$ channels. With the pion-exchange potential we fail to obtain a bound state with the cutoff parameter less than 3.0 GeV. However, when we use the OBE potential and tune the cutoff to be 2.48 GeV, we obtain a bound state with mass 4014.29 MeV. The binding energy is 2.95 MeV and the corresponding root-mean-square radius is 1.61 fm. The channel $D^*D^*(^5S_2)$ with a probability of 99.93% dominates this state.

For the states $D^{(*)}D^{(*)}[I(J^P) = 1(0^+), 1(1^+), 1(2^+)]$, with the present meson exchange approach we can not draw a definite conclusion about whether they are molecules or not. Further detailed study with other approaches are needed.

### 2. $\bar{B}^{(*)}\bar{B}^{(*)}$

With the heavy quark flavor symmetry, the potentials for the $\bar{B}^{(*)}\bar{B}^{(*)}$ system are similar to those for the $DD$ system. The main difference between the two systems is that the reduced mass of the $\bar{B}^{(*)}\bar{B}^{(*)}$ system is much larger than that of the $D^{(*)}D^{(*)}$ system. We summarize our numerical results of the $\bar{B}^{(*)}\bar{B}^{(*)}$ system in Table V.

Similar to the charmed state $D^{(*)}D^{(*)}[I(J^P) = 0(1^+)]$, the bottomed state $\bar{B}^{(*)}\bar{B}^{(*)}[I(J^P) = 0(1^+)]$ is also very interesting. The long-range pion exchange is strong enough to form the loosely bound $\bar{B}^{(*)}\bar{B}^{(*)}[I(J^P) = 0(1^+)]$ state with the cutoff larger than 1.25 GeV. If we tune the cutoff to be 1.30 GeV, the the binding energy is 1.14 MeV and the corresponding root-mean-square radius is 2.25 fm. The channel $[\bar{B}B^*]_-(^3S_1)$ with a probability of 91.83% dominates this state. The probability of the D-wave is 6.96%, see Table V. When we use the OBE potential, the binding becomes tighter as expected, which is similar to its charmed partner $D^{(*)}D^{(*)}[I(J^P) = 0(1^+)]$. With the present meson exchange approach we also suggest that the state $\bar{B}^{(*)}\bar{B}^{(*)}[I(J^P) = 0(1^+)]$ is a good candidate of molecule.

Different from its charmed partner, $\bar{B}^{(*)}\bar{B}^{(*)}[I(J^P) = 0(2^+)]$ can form a bound state with the pion-exchange potential if the cutoff is tuned larger than 2.88 GeV. When we set the cutoff to be 2.88 GeV, the binding energy is 2.75 MeV, and correspondingly, the root-mean-square radius is 0.72 fm. When we use the OBE potential, we obtain the binding solutions with a smaller but more reasonable cutoff. Unfortunately, the binding solutions depend very sensitively on the cutoff parameter. When tune the cutoff from 1.66 GeV to 1.72 GeV, the binding energy changes from 8.30 MeV to 73.89 MeV. The numerical results with the present meson exchange approach suggests that the states $\bar{B}^{(*)}\bar{B}^{(*)}[I(J^P) = 0(2^+)]$ can also be a candidate of molecule, but not a good one because of the strong dependence of the binding solutions on the cutoff.

The pion-exchange alone is also sufficient to form the loosely bound $\bar{B}^{(*)}\bar{B}^{(*)}[I(J^P) = 1(0^+)]$ state with the cutoff larger than 1.70 GeV. When we tune the cutoff from 1.70 GeV to 1.90 GeV, the binding energy increases from 1.05 MeV to 11.29 MeV, and correspondingly, the root-mean-square radius decreases from 2.07 fm to 0.75 fm. The dominant channel is $\bar{B}\bar{B}(^1S_0)$, with a probability of 95.35% $\sim$ 90.29%. And, the probability of the channel $D^*D^*(^5D_0)$ is 1.79% $\sim$ 4.69%. Actually, two pseudoscalar $D$-mesons can not interact with each other via exchanging a pion. Therefore, the binding solutions totally come from the coupled-channel effect, just as in the $\Lambda_Q\Lambda_Q$ case [45, 46]. When we add the contributions of the heavier eta, sigma, rho and omega exchanges, the results change little, which implies that the eta, sigma, rho and omega exchanges cancel with each other significantly. The existence of the state $\bar{B}^{(*)}\bar{B}^{(*)}[I(J^P) = 1(0^+)]$ as a molecule is favored by the present numerical results.

The state $\bar{B}^{(*)}\bar{B}^{(*)}[I(J^P) = 1(1^+)]$ is also an interesting one. When we tune the cutoff between 1.40 GeV and 1.70 GeV, we also obtain a loosely bound state with the OPE potential. The binding energy is 0.83 $\sim$ 11.80 MeV and the corresponding root-mean-square radius is 2.36 $\sim$ 0.80 fm. The dominant channel is $[B\bar{B}^*]_+(^3S_1)$, with a probability of 96.59% $\sim$ 90.63%. Different from the isospin singlet case, when we use the OBE potential the binding becomes shallower. For example, with the OPE potential the binding energy is 11.80 MeV if the cutoff is set to be 1.70 MeV while with the OBE potential it is 8.29 MeV for the same cutoff, see Table V. The present numerical results suggest that $\bar{B}^{(*)}\bar{B}^{(*)}[I(J^P) = 1(1^+)]$ can also be a good candidate of molecule.

With the same reason as for the charmed case, we only keep the three channels $\bar{B}^*\bar{B}^*(^5S_2)$, $\bar{B}^*\bar{B}^*(^1D_2)$ and $\bar{B}^*\bar{B}^*(^5D_2)$ for the state $\bar{B}^{(*)}\bar{B}^{(*)}[I(J^P) = 0(2^+)]$. with the pion-exchange potential, when we tune the cutoff between 1.80 GeV and 2.10 GeV, we obtain a loosely bound state with binding energy 2.25 $\sim$ 13.35 MeV and root-mean-square radius 1.48 $\sim$ 0.71 fm. The dominant channel is $\bar{B}^*\bar{B}^*(^5S_2)$, with a probability of 95.73% $\sim$ 93.66%. When we use the OBE potential and tune the cutoff from 1.70 GeV to 1.76 GeV, the binding energy changes into 7.88 $\sim$ 28.01 MeV, and correspondingly, the root-mean-square radius changes into 0.59 $\sim$ 0.36 fm. The existence of $\bar{B}^{(*)}\bar{B}^{(*)}[I(J^P) = 1(2^+)]$ as a molecule is also favored by our present meson exchange model.

### 3. $D^{(*)}\bar{B}^{(*)}$

The small binding energy and large root-mean-square radius with reasonable cutoff parameter makes the state $D^{(*)}\bar{B}^{(*)}[I(J^P) = 0(0^+)]$ very interesting. With the OPE potential, when we fix the cutoff between 1.08 GeV and 1.20 GeV, we obtain a loosely bound state with binding energy 0.42 $\sim$ 31.35 MeV and root-mean-square radius 4.23 $\sim$ 0.55

TABLE IV: The numerical results for the $D^{(*)}D^{(*)}$ system with strangeness $S = 0$. "×" means the corresponding state dose not exit due to symmetry while "−" means there dose not exist binding energy with the cutoff parameter less than 3.0 GeV. The binding energies for the states $D^{(*)}D^{(*)}[I(J^P) = 0(1^+)]$ and $D^{(*)}D^{(*)}[I(J^P) = 1(1^+)]$ are relative to the threshold of $DD^*$ while that of the state $D^{(*)}D^{(*)}[I(J^P) = 1(0^+)]$ is relative to the $DD$ threshold.

| | | | $D^{(*)}D^{(*)}$ | | | | | | | |
|---|---|---|---|---|---|---|---|---|---|---|
| $I$ | $J^P$ | | OPE | | | | OBE | | | |
| 0 | $0^+$ | | × | | | | × | | | |
| | $1^+$ | $\Lambda$(GeV) | 1.05 | 1.10 | 1.15 | 1.20 | 0.95 | 1.00 | 1.05 | 1.10 |
| | | B.E. (MeV) | 1.24 | 4.63 | 11.02 | 20.98 | 0.47 | 5.44 | 18.72 | 42.82 |
| | | M (MeV) | 3874.61 | 3871.22 | 3864.83 | 3854.87 | 3875.38 | 3870.41 | 3857.13 | 3833.03 |
| | | $r_{rms}$(fm) | 3.11 | 1.68 | 1.12 | 0.84 | 4.46 | 1.58 | 0.91 | 0.64 |
| | | $P_1$(%) | 96.39 | 92.71 | 88.22 | 83.34 | 97.97 | 92.94 | 85.64 | 77.88 |
| | | $P_2$(%) | 0.73 | 0.72 | 0.57 | 0.42 | 0.58 | 0.55 | 0.32 | 0.15 |
| | | $P_3$(%) | 2.79 | 6.45 | 11.07 | 16.11 | 1.41 | 6.42 | 13.97 | 21.91 |
| | | $P_4$(%) | 0.08 | 0.13 | 0.14 | 0.13 | 0.04 | 0.09 | 0.08 | 0.05 |
| | $2^+$ | | - | - | - | - | - | - | - | - |
| 1 | $0^+$ | $\Lambda$(GeV) | - | - | - | - | 2.64 | 2.66 | 2.68 | 2.70 |
| | | B.E.(MeV) | - | - | - | - | 4.29 | 12.63 | 23.30 | 35.75 |
| | | M(MeV) | - | - | - | - | 3730.17 | 3721.83 | 3711.16 | 3698.71 |
| | | $r_{rms}$(fm) | - | - | - | - | 1.38 | 0.79 | 0.58 | 0.48 |
| | | $P_1$(%) | - | - | - | - | 91.47 | 88.26 | 86.25 | 84.80 |
| | | $P_2$(%) | - | - | - | - | 8.46 | 11.64 | 13.63 | 15.07 |
| | | $P_3$(%) | - | - | - | - | 0.07 | 0.10 | 0.12 | 0.13 |
| | $1^+$ | $\Lambda$(GeV) | - | - | - | - | 2.48 | 2.50 | 2.52 | 2.54 |
| | | B.E. (MeV) | - | - | - | - | 0.27 | 3.82 | 9.79 | 17.39 |
| | | M(MeV) | - | - | - | - | 3875.58 | 3872.03 | 3866.06 | 3858.46 |
| | | $r_{rms}$(fm) | - | - | - | - | 5.81 | 1.47 | 0.91 | 0.69 |
| | | $P_2$(%) | - | - | - | - | 99.92 | 99.90 | 99.90 | 99.90 |
| | | $P_3$(%) | - | - | - | - | 0.06 | 0.06 | 0.04 | 0.04 |
| | | $P_4$(%) | - | - | - | - | 0.02 | 0.05 | 0.06 | 0.06 |
| | $2^+$ | $\Lambda$(GeV) | - | - | - | - | 2.48 | 2.50 | 2.52 | 2.54 |
| | | B.E.(MeV) | - | - | - | - | 2.95 | 8.86 | 16.51 | 25.54 |
| | | M(MeV) | - | - | - | - | 4014.29 | 4008.38 | 4000.73 | 3991.70 |
| | | $r_{rms}$(fm) | - | - | - | - | 1.61 | 0.92 | 0.68 | 0.56 |
| | | $P_1$(%) | - | - | - | | 99.93 | 99.94 | 99.95 | 99.95 |
| | | $P_2$(%) | - | - | - | - | 0.01 | 0.01 | 0.01 | 0.00 |
| | | $P_3$(%) | - | - | - | - | 0.06 | 0.05 | 0.04 | 0.04 |

fm. The dominant channel is $D\bar{B}(^1S_0)$, with a probability of 95.32% ∼ 60.03%. The probability of the channel $D^*\bar{B}^*(^5D_0)$ is very small as expected, see Table VI. When we add the contributions of the heavier eta, sigma, rho and omega exchanges, the binding energy changes by tens of MeV. With the present numerical results of the state $D^{(*)}\bar{B}^{(*)}[I(J^P) = 0(0^+)]$, we predict it to be a molecular state.

When the cutoff is tuned larger than 2.05 GeV, the long-range pion exchange is strong enough to form the loosely bound $D^{(*)}\bar{B}^{(*)}[I(J^P) = 0(1^+)]$ state. If we set the cutoff between 2.05 GeV and 2.20 GeV, the binding energy relative to the $D\bar{B}^*$ threshold is 1.21 ∼ 6.30 MeV while the root-mean-square radius is 2.75 ∼ 1.37 fm. The dominant channel is $D\bar{B}^*(^3S_1)$, with a probability of 96.81% ∼ 93.31%. When we add the contributions of the heavier eta, sigma, rho and omega exchanges, we obtain a loosely bound $D^{(*)}\bar{B}^{(*)}[I(J^P) = 0(1^+)]$ state with a reasonable cutoff 1.65 ∼ 1.80 GeV. If we set the cutoff parameter to be 1.70 GeV, the binding energy is 2.83 MeV and the root-mean-square radius is 1.89 fm which is comparable to the size of the deuteron (about 2.0 fm). The channel $D\bar{B}^*(^3S_1)$ with a probability of 95.20% dominates this state. However, the contribution of the D-wave is small, less than 5.0%. It seems that the possibility of $D^{(*)}\bar{B}^{(*)}[I(J^P) = 0(1^+)]$ as a molecule is favored by the present meson exchange approach.

With the same reason as for the state $\bar{B}^{(*)}\bar{B}^{(*)}[I(J^P) = 0(2^+)]$, we omit the channels $D\bar{B}(^1D_2)$, $D\bar{B}^*(^3D_2)$ and $D^*\bar{B}(^3D_2)$ for the state $D^{(*)}\bar{B}^{(*)}[I(J^P) = 0(2^+)]$. Since the amplitudes of the channel $D^*\bar{B}^*(^3D_2)$ scattering into the other channels are zero, we also omit this channel in our study. With the OPE potential, when we set the cutoff between 2.10 GeV and 2.30 GeV, we obtain a bound $D^{(*)}\bar{B}^{(*)}[I(J^P) = 0(2^+)]$

TABLE V: The numerical results the $\bar{B}^{(*)}\bar{B}^{(*)}$ systems with strangeness $S = 0$. "×" means the corresponding state dose not exist due to the symmetry. The binding energies of the states $\bar{B}^{(*)}\bar{B}^{(*)}[I(J^P) = 0(1^+)]$, $\bar{B}^{(*)}\bar{B}^{(*)}[I(J^P) = 0(2^+)]$ and $\bar{B}^{(*)}\bar{B}^{(*)}[I(J^P) = 1(1^+)]$ are relative to the $\bar{B}\bar{B}^*$ threshold while that of the state $\bar{B}^{(*)}\bar{B}^{(*)}[I(J^P) = 1(0^+)]$ is relative to the $\bar{B}\bar{B}$ threshold.

| | | | $\bar{B}^{(*)}\bar{B}^{(*)}$ | | | | | | | |
|---|---|---|---|---|---|---|---|---|---|---|
| $I$ | $J^P$ | | OPE | | | | OBE | | | |
| | $0^+$ | | × | | | | × | | | |
| | | $\Lambda$(GeV) | 1.25 | 1.30 | 1.40 | 1.50 | 1.10 | 1.15 | 1.20 | 1.25 |
| | | B.E. (MeV) | 0.36 | 1.14 | 4.10 | 9.44 | 0.19 | 1.56 | 5.20 | 13.71 |
| | | M (MeV) | 10604.08 | 10603.30 | 10600.34 | 10595.00 | 10604.25 | 10602.88 | 10599.24 | 10590.73 |
| | $1^+$ | $r_{rms}$(fm) | 3.60 | 2.25 | 1.40 | 1.04 | 4.86 | 1.99 | 1.26 | 0.86 |
| | | $P_1$(%) | 94.29 | 91.83 | 89.03 | 83.18 | 96.66 | 94.17 | 92.34 | 86.54 |
| 0 | | $P_2$(%) | 4.16 | 5.66 | 7.01 | 7.10 | 2.61 | 4.04 | 3.54 | 1.96 |
| | | $P_3$(%) | 0.77 | 1.20 | 1.74 | 1.89 | 0.36 | 0.97 | 3.14 | 10.79 |
| | | $P_4$(%) | 0.78 | 1.30 | 2.21 | 2.83 | 0.37 | 0.82 | 0.98 | 0.72 |
| | | $\Lambda$(GeV) | 2.88 | 2.90 | 2.94 | 2.96 | 1.66 | 1.68 | 1.70 | 1.72 |
| | | B.E.(MeV) | 2.75 | 5.18 | 10.38 | 13.15 | 8.30 | 28.01 | 49.89 | 73.89 |
| | $2^+$ | $r_{rms}$ fm | 0.72 | 0.68 | 0.63 | 0.61 | 0.39 | 0.35 | 0.32 | 0.31 |
| | | M(MeV) | 10601.69 | 10599.26 | 10594.06 | 10591.29 | 10596.14 | 10576.43 | 10554.55 | 10530.55 |
| | | $P_1$(%) | 61.15 | 60.47 | 59.43 | 59.01 | 57.82 | 55.86 | 54.69 | 53.88 |
| | | $P_2$(%) | 38.85 | 39.53 | 40.57 | 40.99 | 42.18 | 44.14 | 45.31 | 46.12 |
| | | $\Lambda$(GeV) | 1.70 | 1.75 | 1.80 | 1.90 | 1.74 | 1.76 | 1.78 | 1.80 |
| | | B.E.(MeV) | 1.05 | 2.53 | 4.70 | 11.29 | 2.24 | 8.19 | 15.67 | 24.33 |
| | $0^+$ | M(MeV) | 10557.63 | 10556.15 | 10553.98 | 10547.39 | 10556.44 | 10550.49 | 10543.01 | 10534.35 |
| | | $r_{rms}$(fm) | 2.07 | 1.40 | 1.07 | 0.75 | 1.03 | 0.55 | 0.42 | 0.36 |
| | | $P_1$(%) | 95.35 | 92.82 | 90.29 | 85.46 | 87.27 | 83.59 | 81.81 | 80.66 |
| | | $P_2$(%) | 2.02 | 3.20 | 2.42 | 6.84 | 12.54 | 16.26 | 18.07 | 19.25 |
| | | $P_3$(%) | 2.63 | 3.98 | 5.28 | 7.70 | 0.19 | 0.15 | 0.11 | 0.08 |
| | | $\Lambda$(GeV) | 1.40 | 1.50 | 1.60 | 1.70 | 1.66 | 1.68 | 1.70 | 1.72 |
| | | B.E. (MeV) | 0.83 | 1.89 | 6.46 | 11.80 | 0.55 | 3.72 | 8.29 | 13.92 |
| 1 | $1^+$ | M(MeV) | 10603.61 | 10601.55 | 10597.98 | 10592.64 | 10603.89 | 10600.72 | 10596.15 | 10590.52 |
| | | $r_{rms}$(fm) | 2.36 | 1.38 | 1.00 | 0.80 | 2.26 | 0.85 | 0.59 | 0.48 |
| | | $P_1$(%) | 96.59 | 94.40 | 92.43 | 90.63 | 99.24 | 99.34 | 99.51 | 99.64 |
| | | $P_2$(%) | 1.62 | 2.35 | 2.88 | 3.29 | 0.41 | 0.30 | 0.20 | 0.14 |
| | | $P_3$(%) | 1.79 | 3.25 | 4.69 | 6.08 | 0.34 | 0.36 | 0.29 | 0.22 |
| | | $\Lambda$(GeV) | 1.80 | 1.90 | 2.00 | 2.10 | 1.70 | 1.72 | 1.74 | 1.76 |
| | | B.E.(MeV) | 2.25 | 4.74 | 8.38 | 13.35 | 7.88 | 13.63 | 20.36 | 28.01 |
| | $2^+$ | M(MeV) | 10647.95 | 10645.46 | 10641.82 | 10636.85 | 10642.32 | 10636.57 | 10629.84 | 10622.19 |
| | | $r_{rms}$ | 1.48 | 1.08 | 0.85 | 0.71 | 0.59 | 0.47 | 0.41 | 0.36 |
| | | $P_1$(%) | 95.73 | 94.86 | 94.19 | 93.66 | 99.70 | 99.80 | 99.86 | 99.91 |
| | | $P_2$(%) | 0.72 | 0.87 | 0.97 | 1.06 | 0.05 | 0.03 | 0.02 | 0.01 |
| | | $P_3$(%) | 3.55 | 4.27 | 4.83 | 5.28 | 0.25 | 0.17 | 0.12 | 0.08 |

state, with binding energy 0.80 ∼ 3.83 fm and root-mean-square radius 3.35 ∼ 1.73 fm. The channel $D^*\bar{B}^*(^5S_2)$ provides a dominant contribution, 94.14% ∼ 89.27%. When we use the OBE potential, the binding energy is 0.63 ∼ 1.79 MeV and the root-mean-square radius is 3.70 ∼ 2.43 fm for the cutoff between 1.90 GeV and 2.10 GeV. Such a loosely bound state with weak dependence of the binding solutions on the cutoff parameter is particularly interesting. And, it seems that our present meson exchange model favors the existence of $D^{(*)}B[I(J^P) = 0(2^+)]$ as a molecular state.

For the state $D^{(*)}\bar{B}^{(*)}[I(J^P) = 1(0^+)]$, if we tune the cutoff parameter larger than 2.60 GeV, the OPE potential is sufficient to form the $D^{(*)}\bar{B}^{(*)}[I(J^P) = 1(0^+)]$ bound state. When we fix the cutoff parameter between 2.60 GeV and 2.90 Gev, the binding energy is 0.14 ∼ 17.53 fm and the corresponding root-mean-square radius is 7.05 ∼ 0.75 fm. The dominant channel is $D\bar{B}(^1S_0)$, with a probability of 98.68% ∼ 87.27%. When we use the OBE potential, we obtain binding solutions with a cutoff parameter larger than 2.22 GeV, see Table VI. However, with such a large cutoff parameter, we can not draw a definite conclusion about whether the state $D^{(*)}\bar{B}^{(*)}[I(J^P) = 1(0^+)]$ is a molecule or not. And, further detailed study with other ap-

proach will be helpful to settle this issue.

For the state $D^{(*)}\bar{B}^{(*)}[I(J^P) = 1(1^+)]$, when we tune the cutoff parameter larger than 2.55 GeV, we obtain binding solutions with the OPE potential. If we set the cutoff parameter to be 2.60 GeV, the binding energy relative to the $D\bar{B}^*$ threshold is 2.43 MeV and the corresponding root-mean-square radius is 1.83 fm. However, when we add the heavier eta, sigma, rho and omega exchanges, we obtain no binding solutions with the cutoff parameter less than 3.0 GeV. It seems that the possibility of the state $D^{(*)}\bar{B}^{(*)}[I(J^P) = 1(1^+)]$ as a molecule is ruled out by the present meson exchange model.

For the state $D^{(*)}\bar{B}^{(*)}[I(J^P) = 1(2^+)]$, when we tune the cutoff parameter as large as 2.80 GeV, we obtain binding solutions with the OPE potential. If we set the cutoff parameter to be 2.90 GeV, the binding energy is 2.00 MeV and the corresponding root-mean-square radius is 1.95 fm. The dominant channel is $D^*\bar{B}^*(^5S_2)$, with a probability of 97.56%. The probability of the D-wave is 2.44%. When we use the OBE potential, we obtain binding solutions with a smaller cutoff, see Table VI. If we tune the cutoff to be 2.10 GeV, the binding energy is 0.44 MeV. Similar to the $I(J^P) = 1(0^+)$ case, we can not draw a definite conclusion with such a large cutoff. And, further detailed study with other approach is needed.

### B. The Results for The Systems with Strangeness $S = 1$

For the systems with strangeness $S = 1$, there dose not exist the long-range pion exchange, but there are heavier eta, sigma, $K$ and $K^*$ exchanges. We summarize the our numerical results in Table VII for $(DD)_s$ and $(B\bar{B})_s$ and in Table VIII for $(DB)_s$.

#### 1. $(D^{(*)}D^{(*)})_s$ and $(\bar{B}^{(*)}\bar{B}^{(*)})_s$

When we fix the cutoff parameter between 2.70 GeV and 2.76 GeV, we obtain a bound state of $(D^{(*)}D^{(*)})_s[J^P = 0^+]$ with mass between 3832.06 MeV and 3802.15 MeV and a large root-mean-square radius 1.53 $\sim$ 0.50 fm. The dominant channel is $DD_s(^1S_0)$ with a probability of 92.85% $\sim$ 85.82% and the second largest channel $D^*D^*(^1S_0)$ contributes 7.10% $\sim$ 14.07%. The contribution of the channel $D^*D_s^*(^5D_0)$ is very small, only 0.05% $\sim$ 0.11%. Unfortunately, for such a loosely bound state, we can not draw a definite conclusion with the present meson exchange model about whether it exists as a molecule or not. Now the cutoff parameter is as large as 2.70 GeV which is twice as large as that for the deuteron (1.2 $\sim$ 1.5 GeV [43]) while the binding solutions depend sensitively on the cutoff parameter.

In the corresponding bottomed sector, we also obtain a bound state of $(\bar{B}^{(*)}\bar{B}^{(*)})_s[J^P = 0^+]$ with a smaller and more reasonable cutoff, 1.82 $\sim$ 1.88 GeV. This can be easily understood given that the mass of the bottomed mesons are much larger than those of the charmed mesons and the effective potentials for the two systems are similar. When we tune the cutoff to be 1.82 GeV, the binding energy is 0.56 GeV and the root-mean-square is 2.28 fm which is comparable to that of the deuteron (about 2.0 fm), see Table VII. With the present meson approach, this state can be a candidate of molecular state although not a good one.

The shallow binding solutions and reasonable cutoff parameter (1.44 $\sim$ 1.50 GeV for $(D^{(*)}D^{(*)})_s[J^P = 1^+]$ and 1.10 $\sim$ 1.16 GeV for $(\bar{B}^{(*)}\bar{B}^{(*)})_s[J^P = 1^+]$), make these two states particularly interesting. For the charmed mesons, when we set the cutoff to be 1.44 GeV, the binding energy is 5.43 MeV and the root-mean-square radius is 1.36 fm, see Table VII. The closeness of the thresholds for $DD_s^*$ and $D^*D_s$ makes the channels $DD_s^*(^3S_1)$ and $D^*D_s(^3S_1)$ provide the comparable and main contributions, 45.80% for $DD_s^*(^3S_1)$ and 51.31% for $D^*D_s(^3S_1)$. The D-wave channel $D^*D_s^*(^3D_1)$ and $D^*D_s^*$ provide almost vanishing contributions, 0.02% for $D^*D_s^*(3D_1)$ and 0.00% for $D^*D_s^*(^5D_1)$. This is because of the large mass gap between $D^*D_s^*$ and $D^*D_s$ and the strong repulsive interaction coming from the centrifugal potential of the D-wave. In the bottomed sector, when we fix the cutoff parameter to be 1.10 GeV, the binding energy is 0.67 MeV and the root-mean-square radius is 2.19 fm. Just as in the charmed case, the largest contribution comes from the channels $B\bar{B}_s^*(^3S_1)$ (24.52%) and $\bar{B}^*\bar{B}_s(^3S_1)$ (72.97%). The probabilities of the two channels $\bar{B}^*\bar{B}_s^*(^3D_1)$ and $\bar{B}^*\bar{B}_s^*(^5D_1)$ are negligible, either, with the same reason as for the charmed case. With the present meson exchange approach, it is natural to interpret these two states as molecular states. And, we expect these two states will be studied in the further experiment.

For the state $(D^{(*)}D^{(*)})_s[J^P = 2^+]$, we obtain a bound state with binding energy 1.54 $\sim$ 22.29 MeV when we tune the cutoff to be 2.54 $\sim$ 2.60 GeV. The root-mean square radius is 2.28 $\sim$ 0.60 fm. The dominant channel is $D^*D_s^*(^5S_2)$, with a probability of 99.98%. However, the contributions of the D-wave are negligible. As mentioned before, for such a bound state with a cutoff parameter as large as 2.54 $\sim$ 2.60 GeV, we can not draw a definite conclusion with the present meson exchange model.

For the state $(\bar{B}^{(*)}\bar{B}^{(*)})_s[J^P = 2^+]$, if we fix the cutoff parameter between 1.76 GeV and 1.82 GeV, the binding energy is 0.92 $\sim$ 16.34 MeV and the root-mean-square radius is 1.70 $\sim$ 0.44 fm. The dominant channel is $\bar{B}^*\bar{B}_s^*(^5S_2)$ with a probability of 99.76% $\sim$ 99.85%. The present model also favors (but not strongly) that this state exist as a molecule.

#### 2. $(D^{(*)}\bar{B}^{(*)})_s$

For the state $(D^{(*)}\bar{B}^{(*)})_s[J^P = 0^+]$, if we set the cutoff parameter to be 1.28 GeV, the binding energy is 6.72 MeV and correspondingly, the root-mean-square radius is 0.92 fm. The probability of the channel $D\bar{B}_s(^1S_0)$ is 50.10% while that of the channel $D_s\bar{B}(^1S_0)$ is 25.66%. However, if the binding energy is 68.73 MeV, these two channels provide comparable contributions, 25.30% for $D\bar{B}_s(^1S_0)$ and 23.02% for $D_s\bar{B}(^1S_0)$. Given that the mass gap between $D\bar{B}_s$ and $D_s\bar{B}$ is around 14.5 MeV, for the binding energy comparable to this value, the mass gap plays an important role in the formation of the loosely bound state. However, if the binding energy is as large as 68.73 MeV, which is much larger than the mass gap, the important effect of the mass gap is gone, which is similar

TABLE VI: The numerical results for the $D^{(*)}\bar{B}^{(*)}$ system with strangeness $S = 0$. "–" means we obtain no binding solutions for the corresponding state with the cutoff parameter less than 3.0 GeV. The binding energies of the states $D^{(*)}\bar{B}^{(*)}[I(J^P) = 0(0^+)]$ and $D^{(*)}\bar{B}^{(*)}[I(J^P) = 1(0^+)]$ are relative to the $D\bar{B}^*$ threshold while those of the states $D^{(*)}\bar{B}^{(*)}[I(J^P) = 0(1^+)]$ and $D^{(*)}\bar{B}^{(*)}[I(J^P) = 1(1^+)]$ are relative to the $D\bar{B}$ threshold.

| | | | $D^{(*)}\bar{B}^{(*)}$ | | | | | | | |
|---|---|---|---|---|---|---|---|---|---|---|
| $I$ | $J^P$ | | OPE | | | | OBE | | | |
| 0 | $0^+$ | $\Lambda$(GeV) | 1.08 | 1.12 | 1.16 | 1.20 | 1.00 | 1.02 | 1.04 | 1.06 |
| | | B.E.(MeV) | 0.42 | 5.13 | 15.54 | 31.35 | 1.92 | 6.84 | 15.25 | 27.16 |
| | | M(MeV) | 7146.15 | 7141.15 | 7131.03 | 7115.22 | 7144.65 | 7139.73 | 7131.32 | 7119.41 |
| | | $r_{rms}$(fm) | 4.23 | 1.27 | 0.75 | 0.55 | 2.07 | 1.14 | 0.78 | 0.61 |
| | | $P_1$(%) | 95.32 | 82.45 | 69.99 | 60.03 | 91.21 | 82.14 | 72.93 | 64.72 |
| | | $P_2$(%) | 4.39 | 17.00 | 29.51 | 39.59 | 8.47 | 17.49 | 26.75 | 35.03 |
| | | $p_3$(%) | 0.28 | 0.55 | 0.50 | 0.38 | 0.32 | 0.37 | 0.32 | 0.25 |
| | $1^+$ | $\Lambda$(GeV) | 2.05 | 2.10 | 2.15 | 2.20 | 1.65 | 1.70 | 1.75 | 1.80 |
| | | B.E. (MeV) | 1.21 | 2.44 | 4.13 | 6.30 | 0.44 | 2.83 | 10.75 | 30.86 |
| | | M (MeV) | 7191.12 | 7189.89 | 7188.20 | 7186.03 | 7191.89 | 7189.50 | 7181.58 | 7161.47 |
| | | $r_{rms}$(fm) | 2.75 | 2.02 | 1.63 | 1.37 | 4.37 | 1.89 | 1.05 | 0.65 |
| | | $P_1$(%) | 96.81 | 95.59 | 94.42 | 93.31 | 98.72 | 95.20 | 84.46 | 65.15 |
| | | $P_2$(%) | 0.00 | 0.01 | 0.01 | 0.01 | 0.00 | 0.00 | 0.01 | 0.01 |
| | | $P_3$(%) | 0.22 | 0.30 | 0.38 | 0.46 | 0.26 | 1.49 | 5.96 | 13.96 |
| | | $P_4$(%) | 1.10 | 1.51 | 1.90 | 2.26 | 0.28 | 0.53 | 0.58 | 0.34 |
| | | $P_5$(%) | 0.29 | 0.40 | 0.50 | 0.59 | 0.39 | 2.08 | 8.23 | 20.08 |
| | | $P_6$(%) | 0.38 | 0.52 | 0.67 | 0.80 | 0.09 | 0.20 | 0.24 | 0.16 |
| | | $P_7$(%) | 1.20 | 1.67 | 2.13 | 2.56 | 0.26 | 0.50 | 0.52 | 0.29 |
| | $2^+$ | $\Lambda$(GeV) | 2.10 | 2.15 | 2.20 | 2.30 | 1.90 | 1.95 | 2.00 | 2.10 |
| | | B.E.(MeV) | 0.80 | 1.31 | 1.97 | 3.83 | 0.63 | 0.87 | 1.14 | 1.79 |
| | | M(MeV) | 7332.92 | 7332.41 | 7331.75 | 7329.89 | 7333.09 | 7332.85 | 7332.58 | 7331.93 |
| | | $r_{rms}$(fm) | 3.35 | 2.71 | 2.27 | 1.73 | 3.79 | 3.29 | 2.93 | 2.43 |
| | | $P_1$(%) | 94.14 | 92.83 | 91.58 | 89.27 | 96.83 | 96.41 | 96.03 | 95.36 |
| | | $P_2$(%) | 0.25 | 0.29 | 0.33 | 0.38 | 0.20 | 0.22 | 0.24 | 0.28 |
| | | $P_3$(%) | 5.60 | 6.88 | 8.09 | 10.35 | 2.97 | 3.36 | 3.73 | 4.36 |
| 1 | $0^+$ | $\Lambda$(GeV) | 2.60 | 2.70 | 2.80 | 2.90 | 2.22 | 2.24 | 2.26 | 2.28 |
| | | B.E.(MeV) | 0.14 | 2.56 | 8.27 | 17.53 | 0.62 | 6.64 | 15.45 | 26.01 |
| | | M(MeV) | 7146.43 | 7144 01 | 7138.30 | 7129.04 | 7145.95 | 7139.93 | 7131.12 | 7120.56 |
| | | $r_{rms}$(fm) | 7.05 | 1.78 | 1.04 | 0.75 | 3.05 | 0.87 | 0.57 | 0.45 |
| | | $P_1$(%) | 98.68 | 94.88 | 90.98 | 87.27 | 94.14 | 87.90 | 85.29 | 83.65 |
| | | $P_2$(%) | 0.54 | 2.39 | 4.36 | 6.32 | 5.83 | 12.05 | 14.65 | 16.29 |
| | | $p_3$(%) | 0.66 | 2.73 | 4.66 | 6.41 | 0.03 | 0.05 | 0.06 | 0.06 |
| | $1^+$ | $\Lambda$(GeV) | 2.55 | 2.60 | 2.65 | 2.70 | - | - | - | - |
| | | B.E. (MeV) | 0.94 | 2.43 | 4.67 | 7.67 | - | - | - | - |
| | | M (MeV) | 7191.39 | 7189.90 | 7187.66 | 7184.66 | - | - | - | - |
| | | $r_{rms}$(fm) | 2.87 | 1.83 | 1.35 | 1.08 | - | - | - | - |
| | | $P_1$(%) | 96.13 | 93.82 | 91.53 | 89.31 | - | - | - | - |
| | | $P_2$(%) | 0.00 | 0.01 | 0.01 | 0.01 | - | - | - | - |
| | | $P_3$(%) | 0.99 | 1.64 | 2.33 | 3.03 | - | - | - | - |
| | | $P_4$(%) | 0.70 | 1.09 | 1.45 | 1.77 | - | - | - | - |
| | | $P_5$(%) | 0.92 | 1.48 | 2.03 | 2.57 | - | - | - | - |
| | | $P_6$(%) | 0.26 | 0.41 | 0.54 | 0.66 | - | - | - | - |
| | | $P_7$(%) | 0.99 | 1.56 | 2.12 | 2.66 | - | - | - | - |
| | $2^+$ | $\Lambda$(GeV) | 2.80 | 2.85 | 2.90 | 2.95 | 2.10 | 2.12 | 2.14 | 2.16 |
| | | B.E.(MeV) | 0.49 | 1.11 | 2.00 | 3.17 | 0.44 | 4.64 | 10.86 | 18.45 |
| | | M(MeV) | 7333.23 | 7332.61 | 7331.72 | 7330.55 | 7333.28 | 7329.08 | 7322.86 | 7315.27 |
| | | $r_{rms}$(fm) | 3.80 | 2.57 | 1.95 | 1.58 | 3.51 | 1.03 | 0.68 | 0.54 |
| | | $P_1$(%) | 98.57 | 98.03 | 97.56 | 97.15 | 99.86 | 99.89 | 99.93 | 99.95 |
| | | $P_2$(%) | 0.24 | 0.33 | 0.40 | 0.47 | 0.02 | 0.02 | 0.01 | 0.01 |
| | | $P_3$(%) | 1.20 | 1.65 | 2.04 | 2.38 | 0.12 | 0.09 | 0.06 | 0.04 |

TABLE VII: The numerical results for the $D^{(*)}D^{(*)}/\bar{B}^{(*)}\bar{B}^{(*)}$ systems with strangeness $S = 1$. The binding energy of the state $(D^{(*)}D^{(*)})_s/(\bar{B}^{(*)}\bar{B}^{(*)})_s[J^P = 0^+]$ is relative to the $DD_s$ threshold while that of the state $(D^{(*)}D^{(*)})_s/(\bar{B}^{(*)}\bar{B}^{(*)})_s[J^P = 1^+]$ is relative to the $D^*D_s/\bar{B}^*B_s$ threshold.

| $J^P$ | | $(D^{(*)}D^{(*)})_s$ | | | | $(\bar{B}^{(*)}\bar{B}^{(*)})_s$ | | | |
|---|---|---|---|---|---|---|---|---|---|
| $0^+$ | $\Lambda$(GeV) | 2.70 | 2.72 | 2.74 | 2.76 | 1.82 | 1.84 | 1.86 | 1.88 |
| | B.E.(MeV) | 3.66 | 11.31 | 21.47 | 33.57 | 0.56 | 5.27 | 12.08 | 20.32 |
| | M(MeV) | 3832.06 | 3824.41 | 3814.25 | 3802.15 | 10645.08 | 10640.37 | 10633.56 | 10625.32 |
| | $r_{rms}$(fm) | 1.53 | 0.85 | 0.62 | 0.50 | 2.28 | 0.71 | 0.48 | 0.39 |
| | $P_1$(%) | 92.85 | 89.58 | 87.42 | 85.82 | 92.78 | 86.34 | 83.69 | 82.06 |
| | $P_2$(%) | 7.10 | 10.34 | 12.49 | 14.07 | 7.12 | 13.54 | 16.21 | 17.86 |
| | $p_3$(%) | 0.05 | 0.08 | 0.09 | 0.11 | 0.10 | 0.12 | 0.10 | 0.07 |
| $1^+$ | $\Lambda$(GeV) | 1.44 | 1.46 | 1.48 | 1.50 | 1.10 | 1.12 | 1.14 | 1.16 |
| | B.E. (MeV) | 5.43 | 10.19 | 16.31 | 23.84 | 0.67 | 3.21 | 7.17 | 12.52 |
| | M (MeV) | 3971.68 | 3966.92 | 3960.80 | 3953.27 | 10690.73 | 10688.19 | 10684.23 | 10678.88 |
| | $r_{rms}$(fm) | 1.36 | 1.05 | 0.87 | 0.74 | 2.19 | 1.10 | 0.81 | 0.66 |
| | $P_1$(%) | 45.80 | 47.33 | 47.81 | 47.85 | 24.53 | 36.91 | 41.11 | 42.75 |
| | $P_2$(%) | 0.14 | 0.15 | 0.15 | 0.14 | 0.22 | 0.32 | 0.34 | 0.33 |
| | $P_3$(%) | 51.31 | 48.83 | 47.40 | 46.41 | 72.97 | 58.66 | 52.92 | 49.87 |
| | $P_4$(%) | 0.12 | 0.13 | 0.13 | 0.13 | 0.36 | 0.42 | 0.40 | 0.36 |
| | $P_5$(%) | 2.61 | 3.54 | 4.49 | 5.44 | 1.83 | 3.55 | 5.09 | 6.54 |
| | $P_6$(%) | 0.02 | 0.02 | 0.02 | 0.02 | 0.09 | 0.13 | 0.14 | 0.15 |
| | $P_7$(%) | 0.00 | 0.00 | 0.00 | 0.00 | 0.01 | 0.00 | 0.00 | 0.00 |
| $2^+$ | $\Lambda$(GeV) | 2.54 | 2.56 | 2.58 | 2.60 | 1.76 | 1.78 | 1.80 | 1.82 |
| | B.E.(MeV) | 1.54 | 6.59 | 13.67 | 22.29 | 0.92 | 4.74 | 9.98 | 16.34 |
| | M(MeV) | 4119.38 | 4114.33 | 4107.25 | 4098.63 | 10739.60 | 10735.82 | 10730.52 | 10724.26 |
| | $r_{rms}$(fm) | 2.28 | 1.07 | 0.75 | 0.60 | 1.70 | 0.75 | 0.54 | 0.44 |
| | $P_1$(%) | 99.98 | 99.97 | 99.97 | 99.97 | 99.76 | 99.79 | 99.85 | 99.85 |
| | $P_2$(%) | 0.00 | 0.00 | 0.00 | 0.00 | 0.04 | 0.03 | 0.02 | 0.02 |
| | $P_3$(%) | 0.02 | 0.03 | 0.03 | 0.03 | 0.20 | 0.17 | 0.13 | 0.10 |

to the case of $X(3872)$ [44]. With the present approach we suggest the state $(D^{(*)}\bar{B}^{(*)})_s[J^P = 0^+]$ to be a candidate of the molecule but not a good one due to the strong dependence of the binding solutions on the cutoff parameter.

It is necessary to mention that there exist fourteen channels with the quantum numbers $S, I(J^P) = 1, \frac{1}{2}(1^+)$. It is very hard to solve a $14 \times 14$ matrix Shrödinger equation. Due to the large mass gap between the threshold of $D^*\bar{B}_s^*$(or $D_s^*\bar{B}^*$) and that of $D\bar{B}_s^*$ and the strong repulsive interaction coming from the D-wave, we expect the channels $D^*\bar{B}_s^*(^3D_1)$, $D^*\bar{B}_s^*(^5D_1)$, $D_s^*\bar{B}^*(^3D_1)$ and $D_s^*\bar{B}^*(^5D_1)$ to provide negligible contributions, which can be clearly seen from the previous calculation. Therefore, we omit these four channels in our calculation, which should be a very good approximation. For the state $(D^{(*)}\bar{B}^{(*)})_s[J^P = 1^+]$, it is very interesting that we obtain a loosely bound state with a reasonable cutoff $1.24 \sim 1.30$ GeV. If the cutoff is set to be 1.24 GeV, the binding energy relative to the threshold of $D\bar{B}_s^*$ is 2.50 MeV and the root-mean-square radius is 1.45 fm, see Table VIII. The channel $D\bar{B}_s^*(^3S_1)$ provides the largest contribution, with a probability of 58.10%. The total contribution of the D-wave channels is very small, less than 0.1%, which also proves that our previous approximation is reasonable. With small binding energy and large root-mean-square radius and reasonable cutoff, it is very natural to interpret the state $(D^{(*)}\bar{B}^{(*)})_s[J^P = 1^+]$ as a molecule.

For the state $(D^{(*)}\bar{B}^{(*)})_s[J^P = 2^+]$, if the cutoff parameter is fixed to be 2.20 GeV, the binding energy relative to threshold of $D^*\bar{B}_s^*$ is 1.23 MeV and the root-mean-square radius is 2.25 fm. The dominant channel is $D^*\bar{B}_s^*(^5S_2)$, with a probability of 88.81%. The other S-wave channel $D_s^*\bar{B}^*(^5S_2)$ provides the second largest contribution, 10.90%, and the total contribution of the D-wave is 0.3%. With such a large cutoff, whether the state $(D^{(*)}\bar{B}^{(*)})_s[J^P = 2^+]$ exists as a molecule or not is beyond the present meson exchange model. Further detailed study with other approaches will be helpful to settle this issue.

### C. The Results for The Systems with Strangeness $S = 2$

For the systems with strangeness $S = 2$, there dose not exist the long-range pion exchange, but there are mediate-range sigma and eta exchanges and the short-range phi exchange. We summarize the numerical results for the systems $(D^{(*)}D^{(*)})_{ss}$ and $(\bar{B}^{(*)}\bar{B}^{(*)})_{ss}$ in Table IX and for the system $(D^{(*)}\bar{B}^{(*)})_{ss}$ in Table X.

TABLE VIII: The numerical results of the $D^{(*)}\bar{B}^{(*)}$ system with strangeness $S = 1$. The binding energy of the state $(D^{(*)}\bar{B}^{(*)})_s[J^P = 0^+]$ is relative to the $D\bar{B}_s$ threshold while those of the states $(D^{(*)}\bar{B}^{(*)})_s[J^P = 1^+]$ and $(D^{(*)}\bar{B}^{(*)})_s[J^P = 2^+]$ correspond to the thresholds of $D\bar{B}_s^*$ and $D^*\bar{B}_s^*$ respectively.

| $J^P$ | | $(D^{(*)}\bar{B}^{(*)})_s$ | | | |
|---|---|---|---|---|---|
| $0^+$ | $\Lambda$(GeV) | 1.28 | 1.30 | 1.32 | 1.34 |
| | B.E.(MeV) | 6.72 | 22.10 | 43.11 | 68.73 |
| | M(MeV) | 7226.81 | 7211.43 | 7190.42 | 7164.80 |
| | $r_{rms}$(fm) | 0.92 | 0.55 | 0.43 | 0.36 |
| | $P_1$(%) | 50.10 | 36.04 | 29.33 | 25.30 |
| | $P_2$(%) | 25.66 | 26.98 | 25.07 | 23.02 |
| | $p_3$(%) | 12.03 | 18.55 | 22.96 | 26.05 |
| | $P_4$(%) | 12.06 | 18.30 | 22.56 | 25.58 |
| | $P_5$(%) | 0.07 | 0.05 | 0.04 | 0.03 |
| | $P_6$(%) | 0.08 | 0.06 | 0.04 | 0.03 |
| $1^+$ | $\Lambda$(GeV) | 1.24 | 1.26 | 1.28 | 1.30 |
| | B.E.(MeV) | 2.50 | 14.97 | 32.88 | 54.86 |
| | M(MeV) | 7280.13 | 7267.66 | 7249.75 | 7227.77 |
| | $r_{rms}$(fm) | 1.45 | 0.63 | 0.47 | 0.39 |
| | $P_1$(%) | 19.11 | 23.61 | 22.14 | 20.40 |
| | $P_2$(%) | 58.10 | 35.98 | 28.14 | 23.97 |
| | $P_3$(%) | 4.65 | 8.04 | 9.71 | 10.69 |
| | $P_4$(%) | 4.63 | 8.16 | 9.86 | 10.80 |
| | $P_5$(%) | 6.73 | 11.95 | 14.87 | 16.84 |
| | $P_6$(%) | 6.72 | 12.21 | 15.26 | 17.28 |
| | $P_7$(%) | 0.00 | 0.00 | 0.00 | 0.00 |
| | $P_8$(%) | 0.00 | 0.00 | 0.00 | 0.00 |
| | $P_9$(%) | 0.04 | 0.03 | 0.02 | 0.01 |
| | $P_{10}$(%) | 0.03 | 0.02 | 0.02 | 0.01 |
| $2^+$ | $\Lambda$(GeV) | 2.20 | 2.22 | 2.24 | 2.26 |
| | B.E.(MeV) | 1.23 | 5.68 | 12.65 | 21.29 |
| | M(MeV) | 7422.79 | 7418.34 | 7411.37 | 7402.73 |
| | $r_{rms}$(fm) | 2.25 | 0.95 | 0.62 | 0.49 |
| | $P_1$(%) | 10.90 | 26.64 | 36.08 | 40.94 |
| | $P_2$(%) | 88.81 | 73.18 | 63.83 | 59.01 |
| | $P_3$(%) | 0.02 | 0.01 | 0.01 | 0.00 |
| | $P_4$(%) | 0.01 | 0.00 | 0.00 | 0.00 |
| | $P_5$(%) | 0.18 | 0.12 | 0.06 | 0.03 |
| | $P_6$(%) | 0.09 | 0.05 | 0.02 | 0.01 |

### 1. $(D^{(*)}D^{(*)})_{ss}$ and $(\bar{B}^{(*)}\bar{B}^{(*)})_{ss}$

If we fix the cutoff parameter between 2.76 GeV and 2.82 GeV, we obtain a bound state of $(D^{(*)}D^{(*)})_{ss}[J^P = 0^+]$ with binding energy 2.43 $\sim$ 28.53 MeV and root-mean-square radius 1.92 $\sim$ 0.55 fm. The dominant channel is $D_sD_s(^1S_0)$, with a probability of 94.69% $\sim$ 87.27. The contribution of the D-wave channel $D_s^*D_s^*(^5D_0)$ is very small as expected, less than 0.1%. In the bottomed sector, we obtain binding solutions with a smaller but more reasonable cutoff 1.90 $\sim$ 1.96 GeV. As one can easily read off from Table IX, when we set the cutoff to be 1.90 GeV, the binding energy is 2.27 MeV and the root-mean-square is 1.17 fm. The dominant channel is $\bar{B}_s\bar{B}_s(^1S_0)$, with a probability of 90.83%. However, the D-wave channel $\bar{B}^*\bar{B}^*(^5D_0)$ provides a negligible contribution, 0.29%. Based on the binding solutions, the meson exchange approach favors (but not strongly) that the state $(\bar{B}^{(*)}\bar{B}^{(*)})[J^P = 0^+]$ is a molecule candidate.

For the state $(D^{(*)}D^{(*)})_{ss}[J^P = 1^+]$, when we tune the cutoff parameter between 2.62 GeV and 2.68 GeV, we obtain binding energy 0.41 $\sim$ 16.57 MeV and root-mean-square radius 4.64 $\sim$ 0.71 fm. The dominant channel is $[D_sD_s^*]_+(^3S_1)$, with a probability of 99.98% $\sim$ 99.96%. In the corresponding bottomed case, we obtain a loosely bound state of $(B\bar{B})_{ss}[J^P = 1^+]$ with binding energy 0.83 $\sim$ 11.98 MeV and root-mean-square radius 1.95 $\sim$ 0.54 fm when we set the cutoff parameter between 1.82 GeV and 1.88 GeV. Similar to the charmed case, the dominant channel is $[\bar{B}_s\bar{B}_s^*]_+(^3S_1)$, provid-

ing a contribution 99.41% $\sim$ 99.29%. In our present meson exchange model, the state $(\bar{B}^{(*)}\bar{B}^{(*)})_{ss}[J^P = 1^+]$ can be viewed as a molecule candidate.

For the $J^P = 2^+$ case, the numerical results very similar to those of the $J^P = 1^+$ case, see IX.

### 2. $(D^{(*)}\bar{B}^{(*)})_{ss}$

For the state $(D^{(*)}\bar{B}^{(*)})_{ss}[J^P = 0^+]$, we obtain binding energy 0.64 $\sim$ 21.72 MeV and root-mean-square radius 3.11 $\sim$ 0.52 fm with the cutoff parameter fixed between 2.36 GeV and 2.42 GeV. The channel $D_s\bar{B}_s(^1S_0)$ with a probability of 96.05% $\sim$ 86.20% is the dominant channel. The probability of the channel $D_s^*\bar{B}_s^*(^5D_0)$ is very small, about 0.03%, see Table X.

For the state $(D^{(*)}\bar{B}^{(*)})_{ss}[J^P = 1^+]$, when we fix the cutoff parameter between 2.34 GeV and 2.40 GeV, we obtain binding energy 1.47 $\sim$ 23.41 MeV and corresponding root-mean-square radius 2.02 $\sim$ 0.50 fm. The dominant channel is $D_s\bar{B}_s^*(^3S_1)$, with a probability of 93.37% $\sim$ 83.13%. However, the total contribution of the D-wave is very small, less than 0.1%, see Table X.

Very similar to the $J^P = 0^+$ case, we obtain a bound state of $(D^{(*)}\bar{B}^{(*)})_{ss}[J^P = 2^+]$ with binding energy 2.98 $\sim$ 22.29 MeV and root-mean-square radius 1.35 $\sim$ 0.51 fm. The dominant channel is $D_s^*\bar{B}_s^*(^5S_2)$, with a probability of 99.98%. Based on the present numerical results, whether these three states exist as molecules or not are beyond the present meson exchange approach. Further detailed study with other approaches will be very helpful to settle this issue.

## IV. CONCLUSION

In the present paper, we investigate the possible molecular states composed of two heavy flavor mesons, including $D^{(*)}D^{(*)}$, $\bar{B}^{(*)}\bar{B}^{(*)}$ and $D^{(*)}\bar{B}^{(*)}$ with strangeness $S = 0$, 1 and 2. In our study, we take into account the S-D mixing which plays an important role in the formation of the loosely bound deuteron, and particularly, the coupled-channel effect in the flavor space.

In order to make clear the role of the long-range pion exchange in the formation of the loosely bound states, we give the numerical results with the one-pion-exchange potential for the system with strangeness $S = 0$, as well as the numerical results with the one-boson-exchange potential.

In our study, we notice that the contribution of the D-wave channel with large threshold is almost negligible for the system with a large mass gap among the thresholds of different channels. We also notice that when the binding energy is comparable to or even smaller than the mass gap, the effect of the mass gap will be magnified by the small binding energy, which is similar to the $X(3872)$ case [44].

In the sector with strangeness $S = 0$, our results favor that $D^{(*)}D^{(*)}[I(J^P) = 0(1^+)]$, $\bar{B}^{(*)}\bar{B}^{(*)}[I(J^P) = 0(1^+), 0(2^+), 1(0^+), 1(1^+), 1(2^+)]$ and $D^{(*)}\bar{B}^{(*)}[I(J^P) = 0(0^+), 0(1^+)]$ are good molecule candidates. For these states, the long-range pion exchange is strong enough to from the loosely bound states, and the mediate-range eta and sigma exchanges and the short-range rho and omega exchanges are helpful to strengthen the binding. However, the possibilities of the states $D^{(*)}D^{(*)}[I(J^P) = 0(2^+)]$ and $D^{(*)}\bar{B}^{(*)}[I(J^P) = 1(1^+)]$ as molecules are ruled out by the present meson exchange approach. Whether the states $D^{(*)}D^{(*)}[I(J^P) = 1(0^+), 1(1^+), 1(2^+)]$and $D^{(*)}\bar{B}^{(*)}[I(J^P) = 0(2^+), 1(0^+), 1(2^+)]$ exist as molecules or not are beyond the present meson exchange model. Further detailed study with other approaches will be very helpful to settle this issue.

In the sector with strangeness $S = 1$, from our results the states $(D^{(*)}D^{(*)})_s[I(J^P) = 1^+]$, $(\bar{B}^{(*)}\bar{B}^{(*)})_s[J^P = 1^+]$ and $(D^{(*)}\bar{B}^{(*)})_s[J^P = 0^+, 1^+]$ are good candidates of molecular states. The states $(\bar{B}^{(*)}\bar{B}^{(*)})_s[J^P = 0^+, 2^+]$ may also be molecules, but not strongly favored. Whether the states $(D^{(*)}D^{(*)})_s[J^P = 0^+, 2^+]$ and $(D^{(*)}\bar{B}^{(*)})_s[J^P = 2^+]$ exist as molecules or not are beyond the present meson exchange model, and further study are needed.

For the system with strangeness $S = 2$, our results favor (but not strongly) that the states $(\bar{B}^{(*)}\bar{B}^{(*)})_{ss}[J^P = 0^+, 1^+, 2^+]$ exist as molecules. However, with the present meson exchange model we cannot draw a definite conclusion about whether the states $(D^{(*)}D^{(*)})_{ss}[J^P = 0^+, 1^+, 2^+]$ and $(D^{(*)}\bar{B}^{(*)})_{ss}[J^P = 0^+, 1^+, 2^+]$ are molecules or not, and the further detailed study with other approaches are needed.

It is very interesting to search the predicted exotic hadronic molecular states experimentally. These molecular candidates cannot directly fall apart into the corresponding components due to the absence of the phase space. For these molecular states with double charm, they cannot decay into a double charm baryon plus a light baryon. The masses of the lightest doubly-charmed baryon and light baryon are 3518 MeV and 938 MeV, respectively, corresponding to $\Xi_{cc}^+$ and proton as listed in PDG [41]. The mass of the molecular state is around 3850 MeV and much smaller than the sum of the masses of a doubly-charmed baryon and a light baryon. Therefore such a decay is kinematically forbidden.

However, the heavy vector meson within the exotic molecular state may decay. The $D^*$ mainly decays to $D\pi$ via strong interaction. It also decays into $D\gamma$. Similarly, $D_s^*$, $B^*$ and $B_s^*$ dominantly decay to $D_s\gamma$, $B\gamma$ and $B_s\gamma$ via electromagnetic interaction, respectively. For example, the main decay modes of the exotic double-charm molecular state with one $D^*$ meson are $DD\gamma$ and $DD\pi$. If the molecular candidates contain two heavy pseudoscalar mesons only, they are stable once produced. The $D^*$ meson may also decay via weak interaction. For these exotic molecules with double bottom or both one charm and one bottom, their decay behavior is similar to that of the molecular state with double charm.

The above typical decay modes provide important information to further experimental search. Although very difficult, it is still possible to produce such heavy systems with double bottom or both one charm and one bottom at LHC.

TABLE IX: The numerical results for the $D^{(*)}D^{(*)}/\bar{B}^{(*)}\bar{B}^{(*)}$ systems with strangeness $S = 2$. The binding energy of the state $(D^{(*)}D^{(*)})_{ss}/(\bar{B}^{(*)}\bar{B}^{(*)})_{ss}[J^P = 0^+]$ corresponds to the $D_sD_s/\bar{B}_s\bar{B}_s$ threshold while that of the state $(D^{(*)}D^{(*)})_{ss}/(\bar{B}^{(*)}\bar{B}^{(*)})_{ss}$ corresponds to the threshold of $D_sD_s^*/B_s\bar{B}_s^*$.

| $J^P$ | | $(D^{(*)}D^{(*)})_{ss}$ | | | | $(\bar{B}^{(*)}\bar{B}^{(*)})_{ss}$ | | | |
|---|---|---|---|---|---|---|---|---|---|
| $0^+$ | $\Lambda$(GeV) | 2.76 | 2.78 | 2.80 | 2.82 | 1.90 | 1.92 | 1.94 | 1.96 |
| | B.E.(MeV) | 2.43 | 8.68 | 17.56 | 28.53 | 2.27 | 6.97 | 13.30 | 20.99 |
| | M(MeV) | 3934.55 | 3928.30 | 3919.42 | 3908.45 | 10730.33 | 10725.63 | 10719.30 | 10711.61 |
| | $r_{rms}$(fm) | 1.92 | 1.00 | 0.70 | 0.55 | 1.17 | 0.67 | 0.49 | 0.40 |
| | $P_1$(%) | 94.69 | 91.37 | 89.04 | 87.27 | 90.83 | 87.05 | 84.67 | 83.00 |
| | $P_2$(%) | 5.29 | 8.59 | 10.91 | 12.68 | 8.88 | 12.65 | 15.05 | 16.76 |
| | $p_3$(%) | 0.02 | 0.03 | 0.04 | 0.05 | 0.29 | 0.30 | 0.28 | 0.24 |
| $1^+$ | $\Lambda$(GeV) | 2.62 | 2.64 | 2.66 | 2.68 | 1.82 | 1.84 | 1.86 | 1.88 |
| | B.E. (MeV) | 0.41 | 3.75 | 9.32 | 16.57 | 0.83 | 3.39 | 7.16 | 11.98 |
| | M (MeV) | 4080.38 | 4077.04 | 4071.47 | 4064.22 | 10778.27 | 10775.71 | 10771.94 | 10767.12 |
| | $r_{rms}$(fm) | 4.64 | 1.49 | 0.94 | 0.71 | 1.95 | 0.96 | 0.68 | 0.54 |
| | $P_1$(%) | 99.98 | 99.96 | 99.96 | 99.96 | 99.41 | 99.29 | 99.33 | 99.41 |
| | $P_2$(%) | 0.01 | 0.02 | 0.02 | 0.01 | 0.24 | 0.27 | 0.24 | 0.20 |
| | $P_3$(%) | 0.01 | 0.02 | 0.02 | 0.03 | 0.35 | 0.44 | 0.43 | 0.39 |
| $2^+$ | $\Lambda$(GeV) | 2.60 | 2.62 | 2.64 | 2.66 | 1.82 | 1.84 | 1.86 | 1.88 |
| | B.E.(MeV) | 0.86 | 4.79 | 10.81 | 18.46 | 0.22 | 2.48 | 6.24 | 11.15 |
| | M(MeV) | 4223.74 | 4219.81 | 4213.79 | 4206.14 | 10830.61 | 10828.32 | 10824.62 | 10819.72 |
| | $r_{rms}$(fm) | 3.13 | 1.29 | 0.86 | 0.66 | 3.86 | 1.10 | 0.71 | 0.55 |
| | $P_1$(%) | 99.98 | 99.97 | 99.98 | 99.98 | 99.75 | 99.61 | 99.64 | 99.70 |
| | $P_2$(%) | 0.00 | 0.00 | 0.00 | 0.00 | 0.04 | 0.06 | 0.05 | 0.04 |
| | $P_3$(%) | 0.02 | 0.02 | 0.02 | 0.02 | 0.21 | 0.33 | 0.30 | 0.26 |

## V. ACKNOWLEDGEMENT

This project was supported by the National Natural Science Foundation of China under Grants 11075004, 11021092, 11261130311, 11222547, 11175073, 11035006, Ministry of Science and Technology of China (2009CB825200), the Ministry of Education of China (FANEDD under Grant No. 200924, DPFIHE under Grant No. 20090211120029, NCET, the Fundamental Research Funds for the Central Universities) and the Fok Ying-Tong Education Foundation (No. 131006). This work is also supported in part by the DFG and the NSFC through funds provided to the sinogermen CRC 110 “Symmetries and the Emergence of Structure in QCD”.

[1] N. A. Tornqvist, (2003), arXiv:hep-ph/0308277 [hep-ph].
[2] F. E. Close and P. R. Page, Phys. Lett. **B578**, 119 (2004), arXiv:hep-ph/0309253.
[3] E. S. Swanson, Phys. Lett. **B588**, 189 (2004), arXiv:hep-ph/0311229.
[4] N. A. Tornqvist, Phys. Lett. **B590**, 209 (2004), arXiv:hep-ph/0402237.
[5] X. Liu, X.-Q. Zeng, and X.-Q. Li, Phys. Rev. **D72**, 054023 (2005), arXiv:hep-ph/0507177.
[6] S.-L. Zhu, Phys. Lett. **B625**, 212 (2005), arXiv:hep-ph/0507025.
[7] M. T. AlFiky, F. Gabbiani, and A. A. Petrov, Phys. Lett. **B640**, 238 (2006), arXiv:hep-ph/0506141 [hep-ph].
[8] Y.-R. Liu, X. Liu, W.-Z. Deng, and S.-L. Zhu, Eur. Phys. J. **C56**, 63 (2008), arXiv:0801.3540 [hep-ph].
[9] X. Liu, Y.-R. Liu, W.-Z. Deng, and S.-L. Zhu, Phys. Rev. **D77**, 034003 (2008), arXiv:0711.0494 [hep-ph].
[10] X. Liu, Y.-R. Liu, W.-Z. Deng, and S.-L. Zhu, Phys. Rev. **D77**, 094015 (2008), arXiv:0803.1295 [hep-ph].
[11] C. E. Thomas and F. E. Close, Phys. Rev. **D78**, 034007 (2008), arXiv:0805.3653 [hep-ph].
[12] S. H. Lee, K. Morita, and M. Nielsen, Phys. Rev. **D78**, 076001 (2008), arXiv:0808.3168 [hep-ph].
[13] F. Close and C. Downum, Phys. Rev. Lett. **102**, 242003 (2009), arXiv:0905.2687 [hep-ph].
[14] G.-J. Ding, Phys. Rev. **D79**, 014001 (2009), arXiv:0809.4818 [hep-ph].
[15] G.-J. Ding, J.-F. Liu, and M.-L. Yan, Phys. Rev. **D79**, 054005 (2009), arXiv:0901.0426 [hep-ph].
[16] X. Liu, Z.-G. Luo, Y.-R. Liu, and S.-L. Zhu, Eur. Phys. J. **C61**, 411 (2009), arXiv:0808.0073 [hep-ph].
[17] X. Liu and S.-L. Zhu, Phys. Rev. **D80**, 017502 (2009), arXiv:0903.2529 [hep-ph].
[18] Y.-R. Liu and Z.-Y. Zhang, Phys. Rev. **C79**, 035206 (2009).
[19] S. H. Lee, K. Morita, and M. Nielsen, Nucl. Phys. **A815**, 29 (2009), arXiv:0808.0690 [hep-ph].
[20] P. Ortega, J. Segovia, D. Entem, and F. Fernandez, AIP Conf. Proc. **1257**, 331 (2010).

TABLE X: The numerical results of the $D^{(*)}\bar{B}^{(*)}$ system with strangeness $S = 2$. The binding energy of the state $(D^{(*)}\bar{B}^{(*)})_{ss}[J^P = 0^+]$ is relative to the threshold of $D_s\bar{B}_s$ while that of the state $(D^{(*)}\bar{B}^{(*)})_{ss}[J^P = 1^+]$ corresponds to the $D_s\bar{B}_s^*$ threshold.

| $J^P$ | | $(D\bar{B})_{ss}$ | | | |
|---|---|---|---|---|---|
| $0^+$ | $\Lambda$(GeV) | 2.36 | 2.38 | 2.40 | 2.42 |
| | B.E.(MeV) | 0.64 | 5.16 | 12.43 | 21.72 |
| | M(MeV) | 7334.15 | 7329.63 | 7322.36 | 7313.07 |
| | $r_{rms}$(fm) | 3.11 | 1.06 | 0.68 | 0.52 |
| | $P_1$(%) | 96.05 | 91.15 | 88.25 | 86.20 |
| | $P_2$(%) | 3.94 | 8.82 | 11.72 | 13.17 |
| | $p_3$(%) | 0.02 | 0.03 | 0.03 | 0.03 |
| $1^+$ | $\Lambda$(GeV) | 2.34 | 2.36 | 2.38 | 2.40 |
| | B.E. (MeV) | 1.47 | 6.63 | 14.13 | 23.41 |
| | M (MeV) | 7382.42 | 7377.26 | 7369.76 | 7360.48 |
| | $r_{rms}$(fm) | 2.02 | 0.92 | 0.63 | 0.50 |
| | $P_1$(%) | 93.37 | 88.46 | 85.36 | 83.13 |
| | $P_2$(%) | 0.00 | 0.00 | 0.00 | 0.00 |
| | $P_3$(%) | 3.85 | 6.95 | 9.07 | 10.69 |
| | $P_4$(%) | 0.01 | 0.01 | 0.01 | 0.01 |
| | $P_5$(%) | 2.75 | 4.55 | 5.54 | 6.14 |
| | $P_6$(%) | 0.00 | 0.00 | 0.00 | 0.00 |
| | $P_7$(%) | 0.02 | 0.02 | 0.02 | 0.02 |
| $2^+$ | $\Lambda$(GeV) | 2.26 | 2.28 | 2.30 | 2.32 |
| | B.E.(MeV) | 2.98 | 7.96 | 14.47 | 22.29 |
| | M(MeV) | 7524.72 | 7519.74 | 7513.23 | 7505.41 |
| | $r_{rms}$(fm) | 1.35 | 0.82 | 0.62 | 0.51 |
| | $P_1$(%) | 99.93 | 99.94 | 99.95 | 99.96 |
| | $P_2$(%) | 0.01 | 0.01 | 0.01 | 0.01 |
| | $P_3$(%) | 0.06 | 0.05 | 0.04 | 0.03 |


[21] S. Ohkoda, Y. Yamaguchi, S. Yasui, K. Sudoh, and A. Hosaka, Phys. Rev. **D86**, 014004 (2012), arXiv:1111.2921 [hep-ph].
[22] S. Ohkoda, Y. Yamaguchi, S. Yasui, K. Sudoh, and A. Hosaka, (2012), arXiv:1209.0144 [hep-ph].
[23] F. Aceti, R. Molina, and E. Oset, PoS **QNP2012**, 072 (2012).
[24] M. B. Voloshin and L. B. Okun, JETP Lett. **23**, 333 (1976).
[25] A. De Rujula, H. Georgi, and S. L. Glashow, Phys. Rev. Lett. **38**, 317 (1977).
[26] N. A. Tornqvist, Nuovo Cim. **A107**, 2471 (1994), arXiv:hep-ph/9310225 [hep-ph].
[27] N. A. Tornqvist, Z. Phys. **C61**, 525 (1994), arXiv:hep-ph/9310247.
[28] M. Mattson *et al.*, SELEX Collaboration, Phys. Rev. Lett. **89**, 112001 (2002), arXiv:hep-ex/0208014 [hep-ex].
[29] A. Ocherashvili *et al.*, SELEX Collaboration, Phys. Lett. **B628**, 18 (2005), arXiv:hep-ex/0406033 [hep-ex].
[30] B. Aubert *et al.*, BABAR Collaboration, Phys. Rev. **D74**, 011103 (2006), arXiv:hep-ex/0605075 [hep-ex].
[31] R. Chistov *et al.*, BELLE Collaboration, Phys. Rev. Lett. **97**, 162001 (2006), arXiv:hep-ex/0606051 [hep-ex].
[32] M. B. Wise, Phys. Rev. **D45**, R2188 (1992).
[33] A. F. Falk and M. E. Luke, Phys. Lett. **B292**, 119 (1992), arXiv:hep-ph/9206241 [hep-ph].
[34] B. Grinstein, E. E. Jenkins, A. V. Manohar, M. J. Savage, and M. B. Wise, Nucl. Phys. **B380**, 369 (1992), arXiv:hep-ph/9204207 [hep-ph].
[35] R. Casalbuoni *et al.*, Phys. Rept. **281**, 145 (1997), arXiv:hep-ph/9605342 [hep-ph].
[36] Y.-B. Dai and S.-L. Zhu, Eur. Phys. J. **C6**, 307 (1999), arXiv:hep-ph/9802227 [hep-ph].
[37] F. Navarra, M. Nielsen, M. Bracco, M. Chiapparini, and C. Schat, Phys. Lett. **B489**, 319 (2000), arXiv:hep-ph/0005026 [hep-ph].
[38] S. Ahmed *et al.*, CLEO Collaboration, Phys. Rev. Lett. **87**, 251801 (2001), arXiv:hep-ex/0108013 [hep-ex].
[39] C. Isola, M. Ladisa, G. Nardulli, and P. Santorelli, Phys. Rev. **D68**, 114001 (2003), arXiv:hep-ph/0307367 [hep-ph].
[40] M. Bando, T. Kugo, and K. Yamawaki, Phys. Rept. **164**, 217 (1988).
[41] K. Nakamura and P. D. Group, Journal of Physics G: Nuclear and Particle Physics **37**, 075021 (2010).
[42] I. W. Lee, A. Faessler, T. Gutsche, and V. E. Lyubovitskij, Phys. Rev. **D80**, 094005 (2009), arXiv:0910.1009 [hep-ph].
[43] R. Machleidt, K. Holinde, and C. Elster, Phys. Rept. 149. 1, (1987).
[44] N. Li and S.-L. Zhu, Phys. Rev. **D86**, 074022 (2012), arXiv:1207.3954 [hep-ph].
[45] W. Meguro, Y.-R. Liu, and M. Oka, Phys. Lett. **B704**, 547 (2011), arXiv:1105.3693 [hep-ph].
[46] N. Li and S.-L. Zhu, Phys. Rev. **D86**, 014020 (2012), arXiv:1204.3364 [hep-ph].

## VI. APPENDIX

The functions $H_i$ etc are defined as,

$$
\begin{aligned}
H_0(\Lambda,q_0,m,r) &= \frac{u}{4\pi}\left[Y(ur)-\frac{\chi}{u}Y(\chi r)-\frac{r\beta^2}{2u}Y(\chi r)\right],\\
H_1(\Lambda,q_0,m,r) &= \frac{u^3}{4\pi}\left[Y(ur)-\frac{\chi}{u}Y(\chi r)-\frac{r\chi^2\beta^2}{2u^3}Y(\chi r)\right],\\
H_3(\Lambda,q_0,m,r) &= \frac{u^3}{12\pi}\left[Z(ur)-\frac{\chi^3}{u^3}Z(\chi r)-\frac{\chi\beta^2}{2u^3}Z_2(\chi r)\right],\\
M_1(\Lambda,q_0,m,r) &= -\frac{u^3}{4\pi}\left\{\frac{1}{\theta r}\left[\cos(\theta r)-e^{-\chi r}\right]+\frac{\chi\beta^2}{2\theta^3}e^{-\chi r}\right\},\\
M_3(\Lambda,q_0,m,r) &= -\frac{u^3}{12\pi}\left\{\left[\cos(\theta r)-\frac{3\sin(\theta r)}{\theta r}-\frac{3\cos(\theta r)}{\theta^2 r^2}\right]\right.\\
&\quad\left.\times\frac{1}{\theta r}+\frac{\chi^3}{\theta^3}Z(\chi r)+\frac{\chi\beta^2}{2\theta^3}Z_2(\chi r)\right\}, \qquad (36)
\end{aligned}
$$

where,

$$
\begin{aligned}
\beta^2 &= \Lambda^2-m^2, \qquad & u^2 &= m^2-q_0^2,\\
\theta^2 &= -(m^2-q_0^2), \qquad & \chi^2 &= \Lambda^2-q_0^2,
\end{aligned}
$$

and

$$
\begin{aligned}
Y(x) &= \frac{e^{-x}}{x}, \qquad & Z(x) &= \left(1+\frac{3}{x}+\frac{3}{x^2}\right)Y(x),\\
Z_1(x) &= \left(\frac{1}{x}+\frac{1}{x^2}\right)Y(x), \qquad & Z_2(x) &= (1+x)Y(x).
\end{aligned}
$$

Fourier transformation formulas read:

$$
\begin{aligned}
\frac{1}{u^2+\boldsymbol{q}^2} &\rightarrow H_0(\Lambda,q_0,m,r),\\
\frac{\boldsymbol{q}^2}{u^2+\boldsymbol{q}^2} &\rightarrow -H_1(\Lambda,q_0,m,r),\\
\frac{q_iq_j}{u^2+\boldsymbol{q}^2} &\rightarrow -H_3(\Lambda,q_0,m,r)k_{ij}-\frac{1}{3}H_1(\Lambda,q_0,m,r)\delta_{ij},
\end{aligned} \qquad (37)
$$

where, $k_{ij}=3\frac{r_ir_j}{r^2}-\delta_{ij}$.

We summarize the isospin-dependent coefficients in Tables XI,XII,XIII and the time component of the transferred momentum used in our calculation in Table XIV.

TABLE XI: The isospin-dependent coefficients for the $D^{(*)}D^{(*)}$ and $D^{(*)}\bar{B}^{(*)}$ systems with strangeness $S = 0$. The coefficients of the $\bar{B}^{(*)}\bar{B}^{(*)}$ systems, which are not shown, are similar to those of the $D^{(*)}D^{(*)}$.

| $I = 0$ | $DD$ | $[DD^*]_-$ | $[DD^*]_+$ | $D^*D^*$ |
|---|---|---|---|---|
| $DD$ | $-\frac{3}{2}\rho^a + \frac{1}{2}\omega^a + \sigma^a$ | | | $-\frac{3}{2}\pi^c + \frac{1}{6}\eta^c - \frac{3}{2}\rho^c + \frac{1}{2}\omega^c$ |
| $[DD^*]_-$ | | $-\frac{3}{2}\rho^d + \frac{1}{2}\omega^d + \sigma^d$ | | $\frac{1}{\sqrt{2}}(-\frac{3}{2}\pi^f + \frac{1}{6}\eta^f - \frac{3}{2}\rho^f + \frac{1}{2}\omega^f)$ |
| | | $-(-\frac{3}{2}\pi^e + \frac{1}{6}\eta^e - \frac{3}{2}\rho^e + \frac{1}{2}\omega^e)$ | | $-\frac{1}{\sqrt{2}}(-\frac{3}{2}\pi^g + \frac{1}{6}\eta^g - \frac{3}{2}\rho^g + \frac{1}{2}\omega^g)$ |
| $[DD^*]_+$ | | | $-\frac{3}{2}\rho^d + \frac{1}{2}\omega^d + \sigma^d$ | $\frac{1}{\sqrt{2}}(-\frac{3}{2}\pi^f + \frac{1}{6}\eta^f - \frac{3}{2}\rho^f + \frac{1}{2}\omega^f)$ |
| | | | $+(-\frac{3}{2}\pi^e + \frac{1}{6}\eta^e - \frac{3}{2}\rho^e + \frac{1}{2}\omega^e)$ | $+\frac{1}{\sqrt{2}}(-\frac{3}{2}\pi^g + \frac{1}{6}\eta^g - \frac{3}{2}\rho^g + \frac{1}{2}\omega^g)$ |
| $D^*D^*$ | | | | $-\frac{3}{2}\pi^h + \frac{1}{6}\eta^h - \frac{3}{2}\rho^h + \frac{1}{2}\omega^h + \sigma^h$ |
| $I = 1$ | $DD$ | $[DD^*]_-$ | $[DD^*]_+$ | $D^*D^*$ |
| $DD$ | $\frac{1}{2}\rho^a + \frac{1}{2}\omega^a + \sigma^a$ | | | $\frac{1}{2}\pi^c + \frac{1}{6}\eta^c + \frac{1}{2}\rho^c + \frac{1}{2}\omega^c$ |
| $[DD^*]_-$ | | $\frac{1}{2}\rho^d + \frac{1}{2}\omega^d + \sigma^d$ | | $\frac{1}{\sqrt{2}}(\frac{1}{2}\pi^f + \frac{1}{6}\eta^f + \frac{1}{2}\rho^f + \frac{1}{2}\omega^f)$ |
| | | $-(\frac{1}{2}\pi^e + \frac{1}{6}\eta^e + \frac{1}{2}\rho^e + \frac{1}{2}\omega^e)$ | | $-\frac{1}{\sqrt{2}}(\frac{1}{2}\pi^g + \frac{1}{6}\eta^g + \frac{1}{2}\rho^g + \frac{1}{2}\omega^g)$ |
| $[DD^*]_+$ | | | $\frac{1}{2}\rho^d + \frac{1}{2}\omega^d + \sigma^d$ | $\frac{1}{\sqrt{2}}(\frac{1}{2}\pi^f + \frac{1}{6}\eta^f + \frac{1}{2}\rho^f + \frac{1}{2}\omega^f)$ |
| | | | $+(\frac{1}{2}\pi^e + \frac{1}{6}\eta^e + \frac{1}{2}\rho^e + \frac{1}{2}\omega^e)$ | $+\frac{1}{\sqrt{2}}(\frac{1}{2}\pi^g + \frac{1}{6}\eta^g + \frac{1}{2}\rho^g + \frac{1}{2}\omega^g)$ |
| $D^*D^*$ | | | | $\frac{1}{2}\pi^h + \frac{1}{6}\eta^h + \frac{1}{2}\rho^h + \frac{1}{2}\omega^h + \sigma^h$ |
| $I = 0$ | $D\bar{B}$ | $D\bar{B}^*$ | $D^*\bar{B}$ | $D^*\bar{B}^*$ |
| $D\bar{B}$ | $-\frac{3}{2}\rho^a + \frac{1}{2}\omega^a + \sigma^a$ | | | $-\frac{3}{2}\pi^c + \frac{1}{6}\eta^c - \frac{3}{2}\rho^c + \frac{1}{2}\omega^c$ |
| $D\bar{B}^*$ | | $-\frac{3}{2}\rho^d + \frac{1}{2}\omega^d + \sigma^d$ | $-\frac{3}{2}\pi^e + \frac{1}{6}\eta^e - \frac{3}{2}\rho^e + \frac{1}{2}\omega^e$ | $-\frac{3}{2}\pi^f + \frac{1}{6}\eta^f - \frac{3}{2}\rho^f + \frac{1}{2}\omega^f$ |
| $D^*\bar{B}$ | | | $-\frac{3}{2}\rho^d + \frac{1}{2}\omega^d + \sigma^d$ | $-\frac{3}{2}\pi^g + \frac{1}{6}\eta^g - \frac{3}{2}\rho^g + \frac{1}{2}\omega^g$ |
| $D^*\bar{B}^*$ | | | | $-\frac{3}{2}\pi^h + \frac{1}{6}\eta^h - \frac{3}{2}\rho^h + \frac{1}{2}\omega^h + \sigma^h$ |
| $I = 1$ | $D\bar{B}$ | $D\bar{B}^*$ | $D^*\bar{B}$ | $D^*\bar{B}^*$ |
| $D\bar{B}$ | $\frac{1}{2}\rho^a + \frac{1}{2}\omega^a + \sigma^a$ | | | $\frac{1}{2}\pi^c + \frac{1}{6}\eta^c + \frac{1}{2}\rho^c + \frac{1}{2}\omega^c$ |
| $D\bar{B}^*$ | | $\frac{1}{2}\rho^d + \frac{1}{2}\omega^d + \sigma^d$ | $\frac{1}{2}\pi^e + \frac{1}{6}\eta^e + \frac{1}{2}\rho^e + \frac{1}{2}\omega^e$ | $\frac{1}{2}\pi^f + \frac{1}{6}\eta^f + \frac{1}{2}\rho^f + \frac{1}{2}\omega^f$ |
| $D^*\bar{B}$ | | | $\frac{1}{2}\rho^d + \frac{1}{2}\omega^d + \sigma^d$ | $\frac{1}{2}\pi^g + \frac{1}{6}\eta^g + \frac{1}{2}\rho^g + \frac{1}{2}\omega^g$ |
| $D^*\bar{B}^*$ | | | | $\frac{1}{2}\pi^h + \frac{1}{6}\eta^h + \frac{1}{2}\rho^h + \frac{1}{2}\omega^h + \sigma^h$ |

TABLE XII: The isospin-dependent coefficients for the $(D^{(*)}D^{(*)})_s$ and $(D^{(*)}\bar{B}^{(*)})_s$ systems with strangeness $S = 1$. The coefficients of the $(\bar{B}^{(*)}\bar{B}^{(*)})_s$ systems, which are not shown, are similar to those of the $(D^{(*)}D^{(*)})_s$.

| | $DD_s$ | $DD_s^*$ | $D^*D_s$ | $D^*D_s^*$ |
|---|---|---|---|---|
| $DD_s$ | $\sigma^a + K^{*a}$ | 0 | 0 | $-\frac{1}{3}\eta^c + K^c + K^{*c}$ |
| $DD_s^*$ | | $\sigma^d + K^e + K^{*e}$ | $-\frac{1}{3}\eta^e + K^{*d}$ | $-\frac{1}{3}\eta^f + K^f + K^{*f}$ |
| $D^*D_s$ | | | $\sigma^d + K^e + K^{*e}$ | $-\frac{1}{3}\eta^g + K^g + K^{*g}$ |
| $D^*D_s^*$ | | | | $-\frac{1}{3}\eta^h + \sigma^h + K^h + K^{*h}$ |

| | $D\bar{B}_s$ | $D_s\bar{B}$ | $D\bar{B}_s^*$ | $D_s^*\bar{B}$ | $D^*\bar{B}_s$ | $D_s\bar{B}^*$ | $D^*\bar{B}_s^*$ | $D_s^*\bar{B}^*$ |
|---|---|---|---|---|---|---|---|---|
| $D\bar{B}_s$ | $\sigma^a$ | $K^{*a}$ | 0 | 0 | 0 | 0 | $-\frac{1}{3}\eta^c$ | $K^c + K^{*c}$ |
| $D_s\bar{B}$ | | $\sigma^a$ | 0 | 0 | 0 | 0 | $K^c + K^{*c}$ | $-\frac{1}{3}\eta^c$ |
| $D\bar{B}_s^*$ | | | $\sigma^d$ | $K^e + K^{*e}$ | $-\frac{1}{3}\eta^{*e}$ | $K^{*d}$ | $-\frac{1}{3}\eta^f$ | $K^f + K^{*f}$ |
| $D_s^*\bar{B}$ | | | | $\sigma^d$ | $K^{*d}$ | $-\frac{1}{3}\eta^e$ | $K^g + K^{*g}$ | $-\frac{1}{3}\eta^g$ |
| $D^*\bar{B}_s$ | | | | | $\sigma^d$ | $K^e + K^{*e}$ | $-\frac{1}{3}\eta^g$ | $K^g + K^{*g}$ |
| $D_s\bar{B}^*$ | | | | | | $\sigma^d$ | $K^f + K^{*f}$ | $-\frac{1}{3}\eta^f$ |
| $D^*\bar{B}_s^*$ | | | | | | | $-\frac{1}{3}\eta^h + \sigma^h$ | $K^h + K^{*h}$ |
| $D_s^*\bar{B}^*$ | | | | | | | | $-\frac{1}{3}\eta^h + \sigma^h$ |

TABLE XIII: The isospin-dependent coefficients for the $(D^{(*)}D^{(*)})_{ss}$ and $(D^{(*)}\bar{B}^{(*)})_{ss}$ systems with strangeness $S = 1$. The coefficients of the $(\bar{B}^{(*)}\bar{B}^{(*)})_{ss}$ systems, which are not shown, are similar to those of the $(D^{(*)}D^{(*)})_{ss}$.

| $I = 1$ | $D_sD_s$ | $[D_sD_s^*]_-$ | $[D_sD_s^*]_+$ | $D_s^*D_s^*$ |
|---|---|---|---|---|
| $D_sD_s$ | $\phi^a + \sigma^a$ | 0 | 0 | $\frac{2}{3}\eta^c + \phi^c$ |
| $[D_sD_s^*]_-$ | | $\phi^d + \sigma^d - (\frac{2}{3}\eta^e + \phi^e)$ | $\times$ | $\frac{1}{\sqrt{2}}(\frac{2}{3}\eta^f + \phi^f) - \frac{1}{\sqrt{2}}(\frac{2}{3}\eta^g + \phi^g)$ |
| $[D_sD_s^*]_+$ | | | $\phi^d + \sigma^d + (\frac{2}{3}\eta^e + \phi^e)$ | $\frac{1}{\sqrt{2}}(\frac{2}{3}\eta^f + \phi^f) + \frac{1}{\sqrt{2}}(\frac{2}{3}\eta^g + \phi^g)$ |
| $D_s^*D_s^*$ | | | | $\frac{2}{3}\eta^h + \phi^h + \sigma^h$ |
| | $D_s\bar{B}_s$ | $D_s\bar{B}_s^*$ | $D_s^*\bar{B}_s$ | $D_s^*\bar{B}_s^*$ |
| $D_s\bar{B}_s$ | $\phi^a + \sigma^a$ | 0 | 0 | $\frac{2}{3}\eta^c + \phi^c$ |
| $D_s\bar{B}_s^*$ | | $\phi^d + \sigma^d$ | $\frac{2}{3}\eta^e + \phi^e$ | $\frac{2}{3}\eta^f + \phi^f$ |
| $D_s^*\bar{B}_s$ | | | $\phi^d + \sigma^d$ | $\frac{2}{3}\eta^g + \phi^g$ |
| $D_s^*\bar{B}_s^*$ | | | | $\frac{2}{3}\eta^h + \phi^h + \sigma^h$ |

TABLE XIV: The time component of the transferred momentum, $q_0$, used in our calculation. The other values which are not given are zero.

| $DD$ | | $\bar{B}\bar{B}$ | | $D\bar{B}$ | | | |
|---|---|---|---|---|---|---|---|
| Process | $q_0$ | Process | $q_0$ | Process | $q_0$ | Process | $q_0$ |
| $DD_s \to D_sD$ | $m_{D_s} - m_D$ | $\bar{B}\bar{B}_s \to \bar{B}_s\bar{B}$ | $m_{B_s} - m_B$ | $D_s\bar{B} \to D\bar{B}_s$ | $\frac{(m_{B_s}^2+m_{D_s}^2)-(m_B^2+m_D^2)}{2(m_D+m_{B_s})}$ | $D\bar{B}_s \to D_s\bar{B}$ | $\frac{(m_{B_s}^2+m_{D_s}^2)-(m_B^2+m_D^2)}{2(m_D+m_{B_s})}$ |
| $D_sD \to D_s^*D^*$ | $\frac{(m_{D_s^*}^2+m_D^2)-(m_{D_s}^2+m_{D^*}^2)}{2(m_{D_s^*}+m_{D^*})}$ | $\bar{B}_s\bar{B} \to \bar{B}_s^*\bar{B}^*$ | $\frac{(m_{B_s^*}^2+m_B^2)-(m_{B_s}^2+m_{B^*}^2)}{2(m_{B_s^*}+m_{B^*})}$ | $D_s\bar{B} \to D_s^*\bar{B}^*$ | $\frac{(m_{D_s^*}^2+m_B^2)-(m_{B^*}^2+m_{D_s}^2)}{2(m_{D_s^*}+m_{B^*})}$ | $D_s\bar{B} \to D^*\bar{B}_s^*$ | $\frac{(m_{B_s^*}^2+m_{D_s}^2)-(m_{D^*}^2+m_B^2)}{2(m_{D^*}+m_{B_s^*})}$ |
| $D_sD \to D^*D_s^*$ | $\frac{(m_{D_s^*}^2+m_{D_s}^2)-(m_D^2+m_{D^*}^2)}{2(m_{D^*}+m_{D_s^*})}$ | $\bar{B}_s\bar{B} \to \bar{B}^*\bar{B}_s^*$ | $\frac{(m_{B_s^*}^2+m_{B_s}^2)-(m_{B^*}^2+m_B^2)}{2(m_{B^*}+m_{B_s^*})}$ | $D\bar{B}_s \to D_s^*\bar{B}^*$ | $\frac{(m_{D_s^*}^2+m_{B_s}^2)-(m_D^2+m_{B^*}^2)}{2(m_{D_s^*}+m_{B^*})}$ | $D\bar{B}_s \to D^*\bar{B}_s^*$ | $\frac{(m_{D^*}^2+m_{B_s}^2)-(m_{B_s^*}^2+m_D^2)}{2(m_{D^*}+m_{B_s^*})}$ |
| $D_sD^* \to DD_s^*$ | $\frac{(m_{D_s^*}^2+m_{D_s}^2)-(m_D^2+m_{D^*}^2)}{2(m_D+m_{D_s^*})}$ | $\bar{B}_s\bar{B}^* \to \bar{B}\bar{B}_s^*$ | $\frac{(m_{B_s^*}^2+m_{B_s}^2)-(m_B^2+m_{B^*}^2)}{2(m_B+m_{B_s^*})}$ | $D_s\bar{B}^* \to D\bar{B}_s^*$ | $\frac{(m_{D_s}^2+m_{B_s^*}^2)-(m_D^2+m_{B^*}^2)}{2(m_{D_s}+m_{B^*})}$ | $D_s^*\bar{B} \to D^*\bar{B}_s$ | $\frac{(m_{D_s^*}^2+m_{B_s}^2)-(m_B^2+m_{D^*}^2)}{2(m_{D^*}+m_{B_s})}$ |
| $DD^* \to D^*D$ | $m_{D^*} - m_D$ | $\bar{B}\bar{B}^* \to \bar{B}^*\bar{B}$ | $m_{B^*} - m_B$ | $D\bar{B}^* \to D^*\bar{B}$ | $\frac{(m_{D^*}^2-m_{B^*}^2)-(m_D^2+m_B^2)}{2(m_{D^*}+m_B)}$ | $D^*\bar{B} \to D\bar{B}^*$ | $\frac{(m_{D^*}^2-m_{B^*}^2)-(m_D^2+m_B^2)}{2(m_{D^*}+m_B)}$ |
| $D_sD^* \to D_s^*D$ | $\frac{(m_{D_s^*}^2+m_{D^*}^2)-(m_{D_s}^2+m_D^2)}{2(m_{D_s}+m_{D^*})}$ | $\bar{B}_s\bar{B}^* \to \bar{B}_s^*\bar{B}$ | $\frac{(m_{B_s^*}^2+m_{B^*}^2)-(m_{B_s}^2+m_B^2)}{2(m_{B_s}+m_{B^*})}$ | $D_s\bar{B}^* \to D_s^*\bar{B}$ | $\frac{(m_{D_s^*}^2+m_{B^*}^2)-(m_{D_s}^2+m_B^2)}{2(m_{D_s^*}+m_B)}$ | $D_s^*\bar{B} \to D_s\bar{B}^*$ | $\frac{(m_{B^*}^2+m_{D^*}^2)-(m_B^2+m_D^2)}{2(m_{D_s^*}+m_B)}$ |
| $D_sD^* \to D^*D_s$ | $m_{D^*} - m_{D_s}$ | $\bar{B}_s\bar{B}^* \to \bar{B}^*\bar{B}_s$ | $m_{B^*} - m_{B_s}$ | $D_s\bar{B}^* \to D^*\bar{B}_s$ | $\frac{(m_{B^*}^2+m_{D^*}^2)-(m_{B_s}^2+m_{D_s}^2)}{2(m_{D^*}+m_{B_s})}$ | $D_s^*\bar{B} \to D\bar{B}_s^*$ | $\frac{(m_{D_s^*}^2+m_{B_s^*}^2)-(m_D^2+m_B^2)}{2(m_{D_s^*}+m_B)}$ |
| $DD_s^* \to D_s^*D$ | $m_{D_s^*} - m_D$ | $\bar{B}\bar{B}_s^* \to \bar{B}_s^*\bar{B}$ | $m_{B_s^*} - m_B$ | $D\bar{B}_s^* \to D_s^*\bar{B}$ | $\frac{(m_{B_s^*}^2+m_{D_s^*}^2)-(m_D^2+m_B^2)}{2(m_{D_s^*}+m_B)}$ | $D^*\bar{B}_s \to D_s\bar{B}^*$ | $\frac{(m_{D^*}^2+m_{B^*}^2)-(m_{B_s}^2+m_{D_s}^2)}{2(m_{D_s}+m_{B^*})}$ |
| $DD_s^* \to D^*D_s$ | $\frac{(m_{D_s^*}^2+m_{D^*}^2)-(m_{D_s}^2-m_D^2)}{2(m_{D_s}+m_{D^*})}$ | $\bar{B}\bar{B}_s^* \to \bar{B}^*\bar{B}_s$ | $\frac{(m_{B_s^*}^2+m_{B^*}^2)-(m_B^2+m_{B_s}^2)}{2(m_{B^*}+m_{B_s})}$ | $D\bar{B}_s^* \to D^*\bar{B}_s$ | $\frac{(m_{B_s^*}^2+m_{D^*}^2)-(m_D^2+m_{B_s}^2)}{2(m_D+m_{B_s^*})}$ | $D^*\bar{B}_s \to D\bar{B}_s^*$ | $\frac{(m_{D^*}^2+m_{B_s^*}^2)-(m_{B_s}^2+m_D^2)}{2(m_D+m_{B_s^*})}$ |
| $DD^* \to D^*D^*$ | $\frac{m_{D^*}^2-m_D^2}{4m_{D^*}}$ | $\bar{B}\bar{B}^* \to \bar{B}^*\bar{B}^*$ | $\frac{m_{B^*}^2-m_B^2}{4m_{B^*}}$ | $D\bar{B}^* \to D^*\bar{B}^*$ | $\frac{m_{D^*}^2-m_D^2}{2(m_{D^*}+m_{B^*})}$ | $D^*\bar{B} \to D^*\bar{B}^*$ | $\frac{m_{B^*}^2-m_B^2}{2(m_{D^*}+m_{B^*})}$ |
| $D_sD^* \to D_s^*D^*$ | $\frac{(m_{D_s^*}^2-m_{D_s}^2)}{2(m_{D_s^*}+m_{D^*})}$ | $\bar{B}_s\bar{B}^* \to \bar{B}_s^*\bar{B}^*$ | $\frac{m_{B_s^*}^2-m_{B_s}^2}{2(m_{B_s^*}+m_{B^*})}$ | $D_s\bar{B}^* \to D_s^*\bar{B}^*$ | $\frac{m_{D_s^*}^2-m_{D_s}^2}{2(m_{D_s^*}+m_{B^*})}$ | $D_s^*\bar{B} \to D_s^*\bar{B}^*$ | $\frac{m_{B^*}^2-m_B^2}{2(m_{D_s^*}+m_{B^*})}$ |
| $D_sD^* \to D^*D_s^*$ | $\frac{m_{D_s^*}^2+m_{D_s}^2-2m_{D^*}^2}{2(m_{D^*}+m_{D_s^*})}$ | $\bar{B}_s\bar{B}^* \to \bar{B}^*\bar{B}_s^*$ | $\frac{m_{B_s^*}^2+m_{B_s}^2-2m_{B^*}^2}{2(m_{B^*}+m_{B_s^*})}$ | $D_s\bar{B}^* \to D^*\bar{B}_s^*$ | $\frac{(m_{D^*}^2+m_{B^*}^2)-(m_{D_s}^2+m_{B_s^*}^2)}{2(m_{D^*}+m_{B_s^*})}$ | $D_s^*\bar{B} \to D^*\bar{B}_s^*$ | $\frac{(m_{D_s^*}^2+m_{B_s^*}^2)-(m_{D^*}^2+m_B^2)}{2(m_{D^*}+m_{B_s^*})}$ |
| $DD_s^* \to D_s^*D^*$ | $\frac{2m_{D_s^*}^2-m_D^2-m_{D^*}^2}{2(m_{D_s^*}+m_{D^*})}$ | $\bar{B}\bar{B}_s^* \to \bar{B}_s^*\bar{B}^*$ | $\frac{2m_{B_s^*}^2-m_B^2-m_{B^*}^2}{2(m_{B_s^*}+m_{B^*})}$ | $D\bar{B}_s^* \to D_s^*\bar{B}^*$ | $\frac{(m_{D_s^*}^2+m_{B^*}^2)-(m_D^2+m_{B^*}^2)}{2(m_{D_s^*}+m_{B^*})}$ | $D^*\bar{B}_s \to D_s^*\bar{B}^*$ | $\frac{(m_{D_s^*}^2+m_{B_s}^2)-(m_{D^*}^2+m_{B^*}^2)}{2(m_{D_s^*}+m_{B^*})}$ |
| $DD_s^* \to D^*D_s^*$ | $\frac{m_{D^*}^2-m_D^2}{2(m_{D^*}+m_{D_s^*})}$ | $\bar{B}\bar{B}_s^* \to \bar{B}^*\bar{B}_s^*$ | $\frac{m_{B^*}^2-m_B^2}{2(m_{B^*}+m_{B_s^*})}$ | $D\bar{B}_s^* \to D^*\bar{B}_s^*$ | $\frac{m_{D^*}^2-m_D^2}{2(m_{D^*}+m_{B_s^*})}$ | $D^*\bar{B}_s \to D^*\bar{B}_s^*$ | $\frac{m_{B_s^*}^2-m_{B_s}^2}{2(m_{D^*}+m_{B_s^*})}$ |
| $D_s^*D^* \to D^*D_s^*$ | $m_{D_s^*} - m_{D^*}$ | $\bar{B}_s^*\bar{B}^* \to \bar{B}^*\bar{B}_s^*$ | $m_{B_s^*} - m_{B^*}$ | $D_s^*\bar{B}^* \to D^*\bar{B}_s^*$ | $\frac{(m_{B_s^*}^2+m_{D_s^*}^2)-(m_{B^*}^2+m_{D^*}^2)}{2(m_{D^*}+m_{B_s^*})}$ | $D^*\bar{B}_s^* \to D_s^*\bar{B}^*$ | $\frac{(m_{B_s^*}^2+m_{D_s^*}^2)-(m_{B^*}^2+m_{D^*}^2)}{2(m_{D^*}+m_{B_s^*})}$ |